0026-895X/05/6706-1920–1934$20.00
MOLECULAR PHARMACOLOGY
Copyright © 2005 The American Society for Pharmacology and Experimental Therapeutics
Mol Pharmacol 67:1920–1934, 2005

Vol. 67, No. 6
9423/3031980
Printed in U.S.A.

Identification and Characterization of PDE4A11, a Novel, Widely Expressed Long Isoform Encoded by the Human *PDE4A* cAMP Phosphodiesterase Gene[S]

Derek A. Wallace, Lee Ann Johnston,[1] Elaine Huston, Douglas MacMaster,[2] Thomas M. Houslay, York-Fong Cheung, Lachlan Campbell,[3] Jenni E. Millen,[4] Robin A. Smith, Irene Gall, Richard G. Knowles, Michael Sullivan, and Miles D. Houslay

Molecular Pharmacology Group, Division of Biochemistry and Molecular Biology, Institute of Biomedical & Life Sciences, University of Glasgow, Glasgow, Scotland, United Kingdom (D.A.W., L.A.J., E.H., D.M., T.M.H., Y.-F.C., L.C., J.E.M., I.G., M.D.H.); GlaxoSmithKline, Respiratory Pharmacology, Stevenage, Herts, United Kingdom (R.A.S., R.G.K.); and Astra Charnwood, Loughborough, United Kingdom (M.S.)

Received November 17, 2004; accepted February 24, 2005

ABSTRACT

PDE4A11 is a novel cAMP-specific phosphodiesterase that is conserved in humans, mouse, rat, pig, and bat. Exon-1^{4A11} encodes its unique, 81 amino acid N-terminal region. Reverse-transcriptase polymerase chain reaction performed across the splice junction, plus identification of expressed sequence tags, identifies PDE4A11 as a long isoform possessing UCR1 and UCR2 regulatory domains. Transcript analysis shows that PDE4A11 is widely expressed compared with PDE4A10 and PDE4A4B long isoforms. Truncation analysis identifies a putative promoter in a 250-base pair region located immediately upstream of the start site in Exon-1^{4A11}. Recombinant PDE4A11, expressed in COS-7 cells, is a 126-kDa protein localized predominantly around the nucleus and in membrane ruffles. PDE4A11 exhibits a K_m for cAMP hydrolysis of 4 μM, with relative V_{max} similar to that of PDE4A10 and PDE4A4B. PDE4A11 is dose-dependently inhibited by rolipram, 4-[(3-butoxy-4-methoxyphenyl)-methyl]-2-imidazolidinone (Ro 20-1724), cilomilast, roflumilast, and denbufylline, with IC_{50} values of 0.7, 0.9, 0.03, 0.004, and 0.3 μM, respectively. Soluble and particulate PDE4A11 exhibit distinct rates of thermal inactivation (55°C; $T_{(0.5)}$ = 2.5 and 4.4 min, respectively). Elevating cAMP levels in COS-7 cells activates PDE4A11 concomitant with its phosphorylation at Ser119 by protein kinase A (PKA). PDE4A11 differs from PDE4A4 in sensitivity to cleavage by caspase-3, interaction with LYN SH3 domain, redistribution upon long-term rolipram challenge, and sensitivity to certain PDE4 inhibitors. PDE4A11, PDE4A10, and PDE4A4 all can interact with βarrestin. PDE4A11 is a novel, widely expressed long isoform that is activated by PKA phosphorylation and shows a distinct intracellular localization, indicating that it may contribute to compartmentalized cAMP signaling in cells in which it is expressed.

This work was supported by the Biotechnology and Biological Sciences Research Council and a GlaxoSmithKline CASE research studentship (to D.W.), and by Medical Research Council UK (grant G8604010) and the European Union (grants QLG2-CT-2001-02278 and QLK3-CT-2002-02149) (to M.D.H.).

The nucleotide sequence for PDE4A11 reported in this article has been submitted to the DDBJ/GenBank/EBI Data Bank with accession number AY618547.

[1] Current address: Randox Laboratories Ltd., County Antrim, Northern Ireland, UK.

[2] Current address: CSC, DuPont Teijin Films, Dumfries, UK.

[3] Current address: GlaxoSmithKline, Corporate Intellectual Property, Harlow, Essex, UK.

[4] Current address: EvoQuest Custom Services, Invitrogen, Paisley, UK.

[S] The online version of this article (available at http://molpharm.aspetjournals.org) contains supplemental material.

Article, publication date, and citation information can be found at http://molpharm.aspetjournals.org.

doi:10.1124/mol.104.009423.

The inactivation of the key second-messenger cAMP is achieved through the action of a large multigene family of cyclic nucleotide phosphodiesterases (Beavo and Brunton, 2002; Maurice et al., 2003). Of these, the PDE4 cAMP-specific phosphodiesterase family has attracted considerable attention (Conti et al., 2003; Houslay and Adams, 2003). One reason for this is that PDE4-selective inhibitors act as potent anti-inflammatory agents and are currently being developed to treat various inflammatory diseases, such as chronic obstructive pulmonary disease, asthma, and Crohn's disease (Burnouf and Pruniaux, 2002; Giembycz, 2002). The validity of such approaches has been strongly supported by targeted gene-inactivation studies (Conti et al., 2003; Mehats et al.,

ABBREVIATIONS: PDE, phosphodiesterase; PKA, protein kinase A; ECL, enhanced chemiluminescence; PAGE, polyacrylamide gel electrophoresis; bp, base pair(s); kb, kilobase(s); eGFP, enhanced green fluorescent protein; PCR, polymerase chain reaction; LR2, linker region 2; DMEM, Dulbecco's modified Eagle's medium; PBS, phosphate-buffered saline; KHEM, KCl/EGTA/$MgCl_2$/dithiothreitol/HEPES; HEK, human embryonic kidney; GST, glutathione *S*-transferase; EST, expressed sequence tag; IBMX, 3-isobutyl-1-methylxanthine; ORF, open reading frame; Ro 20-1724, 4-[(3-butoxy-4-methoxyphenyl)-methyl]-2-imidazolidinone; H89, *N*-[2-(4-bromocinnamylamino)ethyl]-5-isoquinoline; Sp1, stimulating protein 1.

2003). In addition, PDE4 isoforms seem to be targeted to interact with specific proteins/lipids in cells (Houslay and Adams, 2003) and, in so doing, play a pivotal role in underpinning the compartmentalization of cAMP signaling (Mongillo et al., 2004).

Four genes (*PDE4A, PDE4B, PDE4C*, and *PDE4D*) generate a large family of PDE4 isoforms through the use of distinct promoters and alternative mRNA splicing (Conti et al., 2003; Houslay and Adams, 2003). Their unique N-terminal regions, each of which is encoded by a specific 5′ exon, thus define individual PDE4 isoforms. PDE4 isoforms are then further subcategorized into either long forms (which possess the regulatory UCR1 and UCR2 modules), short isoforms (which lack UCR1), or supershort isoforms (which lack UCR1 and have a truncated UCR2) (Conti et al., 2003; Houslay and Adams, 2003). The UCR1 module confers susceptibility to activation by PKA-mediated phosphorylation (Sette and Conti, 1996; Hoffmann et al., 1998; MacKenzie et al., 2002), which is believed to provide part of the cellular machinery that allows desensitization to cAMP signaling by accelerating cAMP degradation (Conti et al., 2003). In addition, the UCR1/2 modules serve to orchestrate the functional outcome of extracellular signal-related kinase phosphorylation of the PDE4 catalytic unit (MacKenzie et al., 2000). This is observed for the PDE4B, PDE4C, and PDE4D isoforms but not PDE4A isoforms, whose catalytic unit lacks the consensus site for extracellular signal-related kinase phosphorylation (Baillie et al., 2000).

To date, the human *PDE4A* gene has been shown to encode a short form, called PDE4A1 (Sullivan et al., 1998), the long isoforms PDE4A4B (Bolger et al., 1993) and PDE4A10 (Rena et al., 2001), and a catalytically inactive N- and C-terminally truncated PDE4A7 (Johnston et al., 2004). It is interesting that the PDE4A4B long isoform seems to be up-regulated in macrophages from smokers with chronic obstructive pulmonary disease (Barber et al., 2004), and PDE4A10 has been shown to be up-regulated upon differentiation of monocytes to macrophages (Shepherd et al., 2004). Here, we describe the identification and characterization of a novel, widely expressed PDE4A long isoform, which we call PDE4A11.

Materials and Methods

[^{3}H]cAMP and ECL reagent were from Amersham Biosciences UK, Ltd. (Little Chalfont, Buckinghamshire, UK). Dithiothreitol, *N*-{1-(2,3-dioleoyloxy)propyl}-*N,N,N*,-trimethylammonium methylsulfate, and protease-inhibitor tablets were obtained from Roche Diagnostics (Mannheim, Germany). Bradford reagent was from Bio-Rad (Herts, UK). All other materials were from Sigma Chemical (Poole, Dorset, UK).

SDS/PAGE and Western Blotting. Acrylamide gels (4–12%) were used, and the samples were boiled for 5 min after being resuspended in SDS sample buffer. Gels were run at 100 V/gel for 1 to 2 h with cooling. For detection of transfected PDE by Western blotting, 2- to 50-μg protein samples were separated by SDS-PAGE and then transferred to nitrocellulose before being immunoblotted using the indicated specific antisera. Labeled bands were identified using peroxidase linked to anti-rabbit IgG, and the Amersham ECL Western blotting kit was used as a visualization protocol. We used polyclonal antisera able to detect all active human PDE4A isoforms as described previously (Huston et al., 1996). This was raised against the extreme C-terminal region that is unique to the PDE4A subfamily and which is found in all known active PDE4 isoforms. We also used a polyclonal antiserum (PS54-UCR1-A1) able to detect the (protein kinase A) phosphoserine form of the Arg-Arg-Glu-Ser-Phe motif found in the conserved UCR1 region of all long isoforms (MacKenzie et al., 2002).

Bioinformatics Analyses. The 38-kb region of the human PDE4A gene locus and the 33-kb region of the murine PDE4A gene locus were analyzed by PROSCAN (http://bimas.dcrt.nih.gov/molbio/proscan/), a PolII promoter prediction program, the GRAIL CpG prediction program (http://compbio.ornl.gov/grailexp/), and the GENSCAN exon prediction program (http://genes.mit.edu/GENSCAN.html). Putative transcription factor binding sites within the PDE4A11 promoter were identified using both the online software resource TESS (http://www.cbil.upenn.edu/tess) and TRANSFAC software (http://motif.genome.ad.jp/).

Constructs. The ORF encoding the 860 amino acids of human PDE4A11 (GenBank accession number AY618547), as predicted from the HSPDE4A genomic sequence and cDNA fragments, was engineered for expression in pcDNA3 as done before by us for PDE4A10 (Rena et al., 2001). The S119A mutation of PDE4A11 was generated using the QuikChange site-directed mutagenesis kit (Stratagene, Cambridge, UK) according to the manufacturer's instructions. The presence of the appropriate mutation was confirmed by DNA sequencing as done before by us (Hoffmann et al., 1998; MacKenzie et al., 2002). The expression plasmids encoding PDE4A4B and PDE4A10 isoforms have been described in detail previously (Huston et al., 1996; Sullivan et al., 1998; Rena et al., 2001).

A plasmid encoding PDE4A4B with eGFP fused to its C terminus was used as we described previously (Terry et al., 2003). A plasmid encoding PDE4A11 with eGFP fused at its C terminus, for expression in mammalian cells, was generated using the ORF of PDE4A11 in pcDNA3 as a template for PCR (HotStarTaq DNA Polymerase; QIAGEN, Dorking, Surrey, UK) to incorporate a HindIII site at the 5′ end and a BamHI site at the 3′ end (no STOP to read through GFP). The PCR product was run on low-melting-point agarose gel, band cut-out, and purified (QIAquik Gel Extraction Kit; QIAGEN). This was then ligated (Rapid Ligation Kit; Roche Diagnostics) into HindIII/BamHI-cut pEGFPN1 (BD Biosciences Clontech, Palo Alto, CA). A plasmid encoding PDE4A10 with eGFP fused at its C terminus for expression in mammalian cells was similarly generated. All constructs were confirmed by sequencing.

A putative PDE4A11 promoter construct was formed by cloning a 1-kb fragment immediately upstream of the ATG start for PDE4A11 into the SmaI site of pGL3-Basic (Promega, Madison, WI) to generate p4A11-Luc. Primers corresponding with bases some 750, 500, and 250 bp into the 1-kb PDE4A11 promoter construct were designed. Deletions were PCR-amplified from the 1-kb construct using Platinum Pfx polymerase with PCR conditions of 94°C for 2 min and cycle conditions of 94°C for 15 s, 55°C for 30 s, and 68°C for 1 min. This was repeated up to 45 times, as indicated. The fragments were then cloned using the TOPO TA Cloning Kit (Invitrogen, Carlsbad, CA) according to the manufacturer's protocol. Deletions with the correct orientation were selected using restriction digests. DNA was extracted using the QIAGEN Spin Mini Prep kit according to the manufacturer's protocol. The constructs are referred to by the number of bases that they contain immediately 5′ to the ATG start of PDE4A11 in exon-1^{4A11}. In making these deletions, the reverse primer used was GGCCGCGGGGCGGCCCCGCCTCGGCGGGCG, and the forward primers were GATGGGGAGCTCTGGAGGAATTTTGGGACA (deletion to 750 bp), GAGAGTGCCCTAGGGTTTATGAGGGTGTCT (deletion to 500 bp), and GGCGATTGTGAGGACATTAGAGCCAACGCG (deletion to 250 bp). A PDE4A10 promoter construct consisting of 1 kb of sequence upstream from exon-1^{4A10} and a PDE4A4B promoter construct consisting of 1 kb of sequence upstream from exon-1^{4A4B}, each fused to a luciferase reporter, was formed as we descrived previously (Rena et al., 2001).

TaqMan mRNA Profiles. Leukocytes were isolated from blood samples donated by volunteers at GlaxoSmithKline (Stevenage, UK). Bronchial epithelial and smooth muscle primary cells were

obtained from Cambrex Bio Science Walkersville (Walkersville, MD). Poly A^+ RNA was prepared by the PolyATract method according to manufacturer's instructions (Promega) from the indicated cells of three different individuals. It was then pooled, reverse-transcribed, and analyzed by TaqMan quantitative PCR (Chapman et al., 2000). In brief, 0.5 to 1 μg of poly A^+ RNA was reverse-transcribed using random priming to produce cDNA. Samples were diluted so that wells contained cDNA produced from 1 ng of poly A^+ RNA. TaqMan quantitative PCR (Applied Biosystems, Warrington, UK) was used to assess the level of each gene. A scale-factor normalization method was used to normalize expression against those of three housekeeping genes (cyclophilin, β-actin, and glyceraldehyde-3-phosphate dehydrogenase).

Gene-specific reagents were as follows: for PDE4A4B: forward primer, GGTGTAGGTTGGAAGGGCCA; reverse primer, CAGAGACAGGCTCCTTTCCG; and TaqMan probe, ATGGAACCCCCGACCGTCCCCT; for PDE4A10: forward primer, CCCTGCCCTGGCACT; reverse primer, ACAGATCTGCCCGGAGGGT; and TaqMan probe, CACTTCCCCTTCAGCGATGAGGACACC: for PDE4A11, forward primer, GGCTGAGGACGAGGCGTT; reverse primer, GAAGGCGTCTGCGGAAAGTT; and TaqMan probe, CTCCTCGCCCGTCTTCTTCGCCAG; The housekeeper glyceraldehyde-3-phosphate dehydrogenase forward primer was CAAGGTCATCCATGACAACTTTG, the reverse primer was GGCCATCCACAGTCTTCTGG, and the TaqMan probe was ACCACAGTCCATGCCATCACTGCCA.

RT-PCR Analyses. Amplification of PDE4A11 fragments was carried out using intron-spanning primers. This was done from 2 μg of mRNA using HotStar TaqDNA Polymerase (QIAGEN) and PCR conditions of 50°C for 30 min, 94°C for 15 min, and 35 cycles of 94°C for 1 min, 50°C for 1 min, and 72°C for 1 min. Final extension was carried out at 72°C for 10 min, and the RT-PCR product was visualized by electrophoresis using a 1.2% agarose gel containing ethidium bromide at a final concentration of 0.5 μg/ml. The generic PDE4A fragments were amplified using the sense primer ATGCAGACCTATCGCTCTGTCAGC and the antisense primer ACCATCGTGTCCACAGGGATGC to detect a product of 506 bp, encoding the PDE4A common region, from UCR2 into the catalytic unit. The PDE4A11-specific fragments were generated using the sense primer ATGGCGCGGCCGCGCGGCCTAGGCC and the antisense primers CGGACGCTCCGGAGGCTGGCCAGCACC, to amplify a 497-bp product encoding up to UCR1, or GCGGCTGGGAGGGTCTTGGTCGCGGCGC, to amplify an 886-bp product encoding up to linker region 2 (LR2).

To assess the human tissue expression of PDE4A11, a panel of first-strand cDNAs prepared from 24 human tissues (OriGene Technologies Inc., Rockville, MD) was used according to the manufacturer's instructions. These were used as PCR templates to generate a 494-bp fragment using the sense primer GGAGCTGCAACTGGTGGC, designed to the unique N-terminal region of PDE4A11, and the antisense primer GGCACATTGGTCAGGAGTGAG, designed to the nucleotide sequence encoding LR1. The PCR analysis was done using HotStar TaqDNA Polymerase (QIAGEN), and PCR conditions were 95°C for 15 min and 35 cycles of 95°C for 30 s, 50°C for 30 s, and 72°C for 1 min. Final extension was carried out at 72°C for 10 min, and the PCR product was visualized as described above.

Transient Expression of PDE4 Isoforms in COS-7 Cells. Transfection was done using the COS-7 SV40-transformed monkey kidney cell line maintained at 37°C in an atmosphere of 5% CO_2/95% air in complete growth medium containing DMEM supplemented with 0.1% penicillin/streptomycin (10,000 units/ml), 2 mM glutamine, and 10% fetal calf serum. We have described this before in some detail (Huston et al., 1996; McPhee et al., 1999; Rena et al., 2001). In brief, COS-7 cells were transfected using DEAE-dextran. The DNA to be transfected (10 μg) was mixed and incubated for 15 min with 200 μl of 10 mg/ml DEAE-dextran in PBS to give a "DNA-dextran" mix. When cells reached 70% confluence in 100-mm dishes, the medium was removed, and the cells were given 10 ml of fresh DMEM containing 0.1 mM chloroquine and the DNA-dextran mix (450 μl). The cells were then incubated for 4 h at 37°C. After this period, the medium was removed, and the cells were shocked with 10% dimethyl sulfoxide in PBS. After PBS washing, the cells were returned to normal growth medium and left for an additional 2 days before use. For determination of PDE activity, the cells were homogenized in KHEM buffer (50 mM KCl, 10 mM EGTA, 1.92 mM $MgCl_2$, 1 mM dithiothreitol, and 50 mM HEPES; final pH, 7.2) containing "complete" protease inhibitors (Roche Diagnostics) of final concentrations 40 μg/ml phenylmethylsulfonyl fluoride, 156 μg/ml benzamine, 1 μg/ml aprotonin, 1 μg/ml leupeptin, 1 μg/ml pepstatin A, and 1 μg/ml antipain. As described previously (Huston et al., 1996; Sullivan et al., 1998; Rena et al., 2001) in such transfected cells, then >98% of the total PDE activity was caused by the recombinant PDE4 isoform. In some instances, the transfected COS-7 cells were plated onto six-well plates for use in experiments and then serum-starved overnight before being treated with the indicated ligands for the stated lengths of time.

Luciferase Reporter Assays. Human embryonic kidney (HEK) 293 cells were transfected using Transfast Transfection Reagent (Promega) and cotransfected with 1.2 μg of firefly luciferase and 0.12 μg of the control *Renilla reniformis* luciferase construct pRL-CMV (Promega). The appropriate plasmids were then mixed with 45 μl of serum-free medium and 4 μl of Transfast reagent. After a 10-min incubation at room temperature, 40 μl of DNA mix was added to the cells and incubated for 1 h at 37°C. They were then overlaid with 200 μl of DMEM. Then, 48 h after transfection, the cells were lysed and assayed using the Dual Luciferaser Reporter Assay system (Promega) as described in the manufacturer's protocol using a Packard

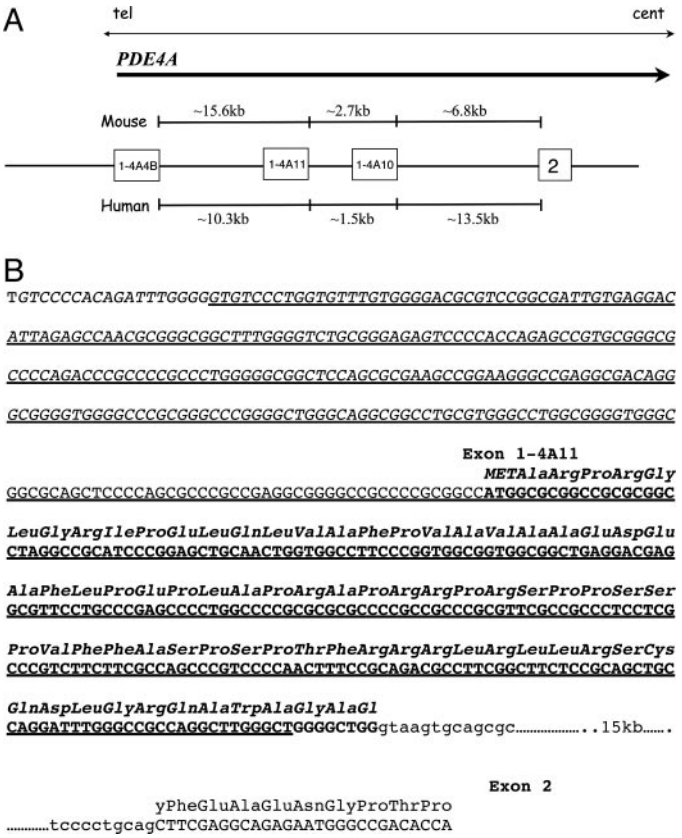

Fig. 1. Schematic representation of the disposition of unique 5′ exons in the PDE4A gene. A, organization of the unique 5′ exons (exon-1) that encode the N-terminal regions of the PDE4A4B, PDE4A10, and novel PDE4A11 isoforms in the *PDE4A* gene as well as the first common exon (exon-2) used by all these three long isoforms. B, human genomic sequence showing exon-1 of the PDE4A11 splice variant. Nucleotides in boldface show the coding region of exon-1^{4A11}. The nucleotide sequence underlined is the region identified as a CpG-rich island.

Fusion Universal Microplate Analyzer (PerkinElmer Life and Analytical Sciences, Boston, MA). Luciferase activity values were normalized against the *R. reniformis* internal control.

Confocal Analyses. PDE4A11 was transiently overexpressed and visualized in COS cells using PDE4A-specific antisera as described previously by us for analyses of PDE4A4B (Huston et al., 1996; McPhee et al., 1999). In brief, cells were transfected using *N*-{1-(2,3-dioleoyloxy)propyl}-*N*,*N*,*N*,-trimethylammonium methylsulfate (Roche Diagnostics) with the PDE4A11-pcDNA3 plasmid. Protein was expressed for 48 h, and cells were fixed in 4% paraformaldehyde containing 5% sucrose. After permeabilization in 0.2% Triton X-100, proteins were blocked using 10% goat serum and 2% bovine serum albumin before PDE4A11 was detected using an antibody raised against the C terminus of human PDE4A and stained using Alexa 594 (Molecular Probes, Eugene, OR). Cells were observed using a Zeiss Pascal laser-scanning microscope (Carl Zeiss GmbH, Jena, Germany).

For studies done on living cells, GFP chimeras of PDE4A4B and PDE4A11 were used. COS cells were transfected with plasmids encoding in-frame fusions of either PDE4A4-GFP or PDE4A11-GFP using Fugene 6 (Roche Diagnostics). Proteins were expressed for 32 h before rolipram (10 μM) was added to the cells for a further 16 h, essentially as described previously by us (Terry et al., 2003). PDE4A4-GFP and PDE4A11-GFP localization was examined using a Zeiss Pascal laser-scanning microscope.

Interaction with the SH3 Domain of LYN and with β-Arrestin. Assessment of the interaction of PDE4A11, PDE4A4, and PDE4A10 with the SH3 domain of LYN, expressed in *Escherichia coli* and subsequently purified to homogeneity, was done exactly as described in some detail previously by us for PDE4A10 (Rena et al., 2001) and other PDE4 species (McPhee et al., 1999; Huston et al., 2000). In brief, volumes of slurry containing 400 μg of the fusion protein immobilized on glutathione agarose beads were pelleted, and the supernatants were discarded. Within each assay, volumes taken were equalized with washed beads. The pellets were resuspended in the cytosol from COS-7 cells that had been transiently transfected to express the indicated PDE4A form. To allow for the binding of these various PDE4A long isoforms to LYN-SH3 to be compared, an amount of cytosol fraction containing equal amounts of these enzymes, as assessed immunologically with PDE4A-specific antisera, was taken. The amount of PDE4A4 was chosen such that approximately 80% became bound to LYN-SH3; this was usually of the order of 200 μg of lysate protein. These were diluted to a final volume of 200 μl in KHEM buffer containing 1 mM dithiothreitol and protease inhibitor cocktail. The immobilized fusion protein and cytosol were incubated together for 10 min end-over-end at 4°C. The beads were then collected by centrifugation, and the supernatant was retained as the unbound fraction. The beads were held on ice and washed three times with 400 μl of KHEM containing 1 mM dithiothreitol and protease inhibitor cocktail over a 15-min period. These washes were pooled along with the unbound fraction and aliquots taken for Western blotting, along with the bead-bound PDE. This same method was used to determine the putative interaction of the various PDE4A long isoforms with β-arrestin as described previously in some detail for PDE4D isoforms using a purified β-arrestin2-GST fusion protein generated in *E. coli* with recombinant PDE4A isoforms expressed in COS-7 cells (Perry et al., 2002; Bolger et al., 2003).

Action of Caspase-3 on PDE4A Isoforms. Recombinant caspase-3 was generated in an active form as described before (Huston et al., 2000). Cytosolic COS-7 cell lysate (10 μg) expressing the indicated PDE4A isoforms was incubated for 2 h at 37°C with recombinant caspase-3 as described previously by us (Huston et al., 2000). To normalize for the amount of mature caspase-3, in each instance, an equal concentration (147 ng) of the p20 active caspase-3 subunit was added in a final volume of 25 μl of complete KHEM. Resultant protein was boiled in SDS sample buffer solution for Western blotting and probed with either an antibody raised to the common C-terminal region of PDE4A or an antibody specific to the N-terminal region of PDE4A4 (and PDE4A5) (Huston et al., 2000).

Assay of cAMP PDE Activity. PDE activity was determined by a two-step procedure using 1 μM cAMP as substrate, as described previously by us in some detail (Huston et al., 1996; Sullivan et al., 1998; Rena et al., 2001). All assays were conducted at 30°C, with initial rates taken from linear time courses. Activity was linear with added protein concentration.

Protein Analysis. Protein concentration was determined using bovine serum albumin as standard.

TABLE 1

The bioinformatic identification and analysis of PDE4A11 ESTs from various species

Shown are the GenBank descriptors for ESTs that encode either PDE4A11, PDE4A4B, or PDE4A10 by virtue of their having the appropriate exon-1 sequence. Also shown is whether such ESTs have sequence representing *PDE4A* downstream exons. The largest of these ESTs for PDE4A11 extends from exon-1 down to exon-8, which lies in the PDE4A catalytic unit (CA775139).

Acc. No.	Species	4A4B	4A11	4A10	Exon 2	Exon 3	Exon 4	Exon 5	Exon 6	Exon 7	Exon 8
BF346277	Human	Yes			Yes	Yes	Yes				
BY015160	Mouse	Yes									
BY124416	Mouse	Yes									
CA775139	Human		Yes		Yes	Yes	Yes	Yes	Yes	Yes	Yes
AW104482	Human		Yes		Yes	Yes	Yes	Yes	Yes		
CA774868	Human		Yes		Yes	Yes	Yes	Yes	Yes	Yes	
BI438716	Human		Yes		Yes	Yes	Yes	Yes			
BF732322	Human		Yes								
BF116176	Human		Yes								
AW296744	Human		Yes								
BI156706	Mouse		Yes		Yes						
BY352528	Mouse		Yes		Yes						
BY184004	Mouse		Yes		Yes						
BY183996	Mouse		Yes		Yes						
BY353288	Mouse		Yes		Yes						
BY209230	Mouse		Yes		Yes						
BY352150	Mouse		Yes		Yes						
BY347207	Mouse		Yes		Yes						
BX921915	Pig		Yes		Yes						
BF300255	Mouse			Yes	Yes	Yes	Yes	Yes	Yes		
CK795128	Mouse			Yes	Yes						
BY748490	Mouse			Yes	Yes						
BY749598	Mouse			Yes	Yes						
BE531640	Mouse			Yes	Yes						
CK482793	Rat			Yes	Yes						

Results

The human PDE4A gene locus is located at chromosome 19p13.2 (Sullivan et al., 1998). Our sequencing and subsequent analysis (Sullivan et al., 1998) of a chromosome 19 cosmid contig containing the PDE4A gene locus led us to suggest that it may contain a hitherto unknown PDE4A long isoform. This was taken from the finding of a sequence previously found in a cDNA clone, called TM3, which had been postulated to encode a catalytically inactive, C-terminally truncated protein (Bolger, 1994). However, the extreme 3′ 360 bp of the TM3 clone is not found in the human genome database. Indeed, it has been concluded (Sullivan et al., 1998) that this "alien" sequence reflects the inverted 3′ end of the pM5 cDNA. It is therefore likely that the TM3 clone is composed of two unrelated cDNAs that became inappropriately ligated during cloning. Thus, the suggestion (Bolger et al., 1993) that TM3 reflects a truncated, catalytically inactive product of the PDE4A gene is, we believe, incorrect. The portion of the TM3 cDNA sequence found in the PDE4A-containing contig is located between the single unique 5′ exons that encode the PDE4A4B and PDE4A10 long isoforms (Fig. 1). As such, it is appropriately positioned to provide a novel PDE4A long isoform. The prediction of this is that transcripts from any such novel long isoform, which we call here PDE4A11, should show sequence from the 5′ exon spliced directly onto exon-2 of the PDE4A gene rather than to more distant 3′ exons characteristic of short and supershort isoforms.

Comparative Genomics Analysis of the Human and Murine PDE4A Gene Loci. The 38-kb region of the human PDE4A gene locus and the 33-kb region of the murine PDE4A gene locus were analyzed by PROSCAN (http://bimas.dcrt.nih.gov/molbio/proscan/), a PolII promoter prediction program, the GRAIL CpG prediction program (http://compbio.ornl.gov/grailexp/), and the GENSCAN exon prediction program (http://genes.mit.edu/GENSCAN.html). Such comparative genomic analysis allowed us to identify a 5′ exon for PDE4A11 (Fig. 1A) that contained sequence found in the PDE4A11 (TM3) cDNA (Fig. 1B). Also identified were sequences immediately 5′ to the exon-1^{4A11} that are conserved in human and mouse genes, which may be indicative of a functional promoter controlling PDE4A11 expression (see below).

The nucleotide sequence of exon-1^{4A11} was used to interrogate, using the BLAST algorithm, the expressed sequence tag (EST) database and high-throughput sequence nucleotide databases. This allowed us to identify PDE4A11 sequences from various species, namely two mouse genomic draft sequences (GenBank accession numbers AC027154 and AC073749), one rat genomic draft sequence (GenBank accession number AC115140), seven human EST cDNAs (GenBank accession numbers BI438716, BF732322, BF116176, AW296744, AW104482, CA775139, and CA774868), eight mouse EST cDNAs (GenBank accession number BI56706, BY352528, BY184004, BY183996, BY353288, BY209230, BY352150, and BY347207), one bat EST cDNA (GenBank accession number AC148813), and one pig EST cDNA (GenBank accession number BX921915). All of these contained sequence showing high homology to that of the novel human PDE4A11-specific 5′ sequence we identified here (Table 1). However, it is clear (Table 1) that four of the human EST cDNAs (BI438716, AW104482, CA775139, and CA774868) also contained authentic sequence of human exons-2, -3, -4, and –5, three extended to exon-6, two to exon-7, and one to exon-8 within the catalytic unit (Table 1). These data clearly demonstrate splicing of the unique PDE4A11 5′ exon-1 to the first long form exon, namely exon-2, indicating that PDE4A11 is indeed an authentic PDE4A long isoform. Consistent with this, inspection of the sequence of all of the murine ESTs similarly shows splicing onto the murine exon-2 (Table 1). In addition, the murine EST BI156706 showed a 98% match with the draft murine genomic sequence, and analysis of the flanking genomic sequence revealed a consensus 5′ splice-acceptor site. Indeed, comparison of these human and murine PDE4A11 unique 5′ sequences clearly revealed a conserved initiating methionine residue that predicts an in-frame ORF when spliced onto the common exon-2 (Table 1). Comparison (Fig. 2) of the human and mouse unique PDE4A11 N-terminal regions reveals clear conservation between species; however, this is clearly less than the 100% conservation seen for the human and murine unique N-terminal regions of PDE4A1 (Sullivan et al., 1998), PDE4A4 (Bolger et al., 1993; Huston et al., 1996; Sullivan et al., 1998), and PDE4A10 (Rena et al., 2001). Indeed, although the human PDE4A11 unique N-terminal region consists of 81 amino acids, that of murine PDE4A11 consists of only 66 amino acids (Fig. 2).

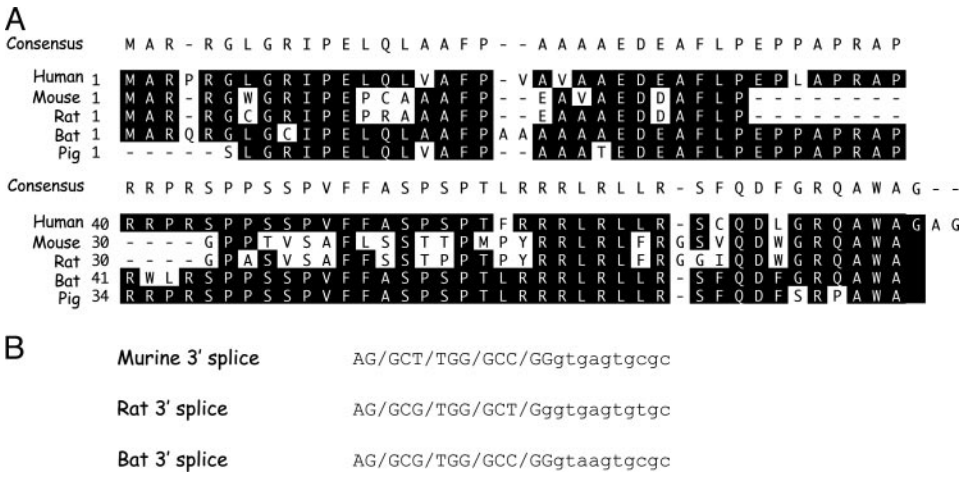

Fig. 2. Alignments of the predicted amino acid sequence encoded by the PDE4A11 unique 5′ exon from various species. A, alignments are shown for the amino acid sequence encoded by cognate PDE4A11 5′ exons found in genomic sequences from human (GenBank accession number AC011548), bat (GenBank accession number AC148813), mouse (GenBank accession numbers AC027154 and AC073749), and rat (GenBank accession number AC148813). B, the sequences for the authentic 3′ splice sites for mouse, rat, and bat are shown.

Expression Profile of PDE4A11. A schematic of the structure of PDE4 isoforms and the exons that encode it is shown in Fig. 3A. The unique 5′ exon of human PDE4A11 encodes the 81 amino acid unique N-terminal region of this isoform, whereas exons-2 to -15 encode the regulatory UCR1/2, the catalytic region, and C-terminal portion (Fig. 3A). Using human brain RNA, we were able to use RT-PCR to amplify from the unique 5′ region of PDE4A11 into either the common UCR1 found only in full-length PDE4 long isoforms and into LR2, which abuts the catalytic unit (Fig. 3B). We were also able to detect transcripts for PDE4A11 in RNA from HEK293 cells using RT-PCR to amplify from the unique 5′ region of PDE4A11 into the common UCR1 found only in full-length PDE4 long isoforms (Fig. 3B). This ability to undertake RT-PCR across the long-form splice junction and into UCR1 confirms the EST data (Table 1) in identifying transcripts for PDE4A11 as a novel PDE4A long isoform.

We screened (Fig. 4A) a panel of RNA from various human tissues by RT-PCR using a sense primer targeted within the unique region of PDE4A11 and an antisense primer targeted within LR2 (Fig. 3A). This analysis identified transcripts for PDE4A11 in a variety of human tissues (Fig. 4A). The size of the transcript and its sequence (data not shown) confirmed PDE4A11 as a long isoform because amplification was achieved across the conserved long form splice junction so as to encompass both UCR1 and UCR2 (Fig. 3A). Transcripts were most abundant in liver, stomach, testis, thyroid, and adrenal glands but were clearly evident in placenta, kidney, pancreas, ovary, uterus, and skin (Fig. 5a). It is interesting that although a clear signal for PDE4A11 transcripts was seen in fetal brain, little signal was seen in adult brain (Fig. 4A). This might indicate a developmental change in PDE4A11 expression in brain and contrasts with PDE4A10, which is seemingly absent from fetal brain but is seen clearly in adult brain (Rena et al., 2001). Indeed, PDE4A10 and PDE4A11 seem to show very distinct patterns of distribution (Fig. 4A) (Rena et al., 2001).

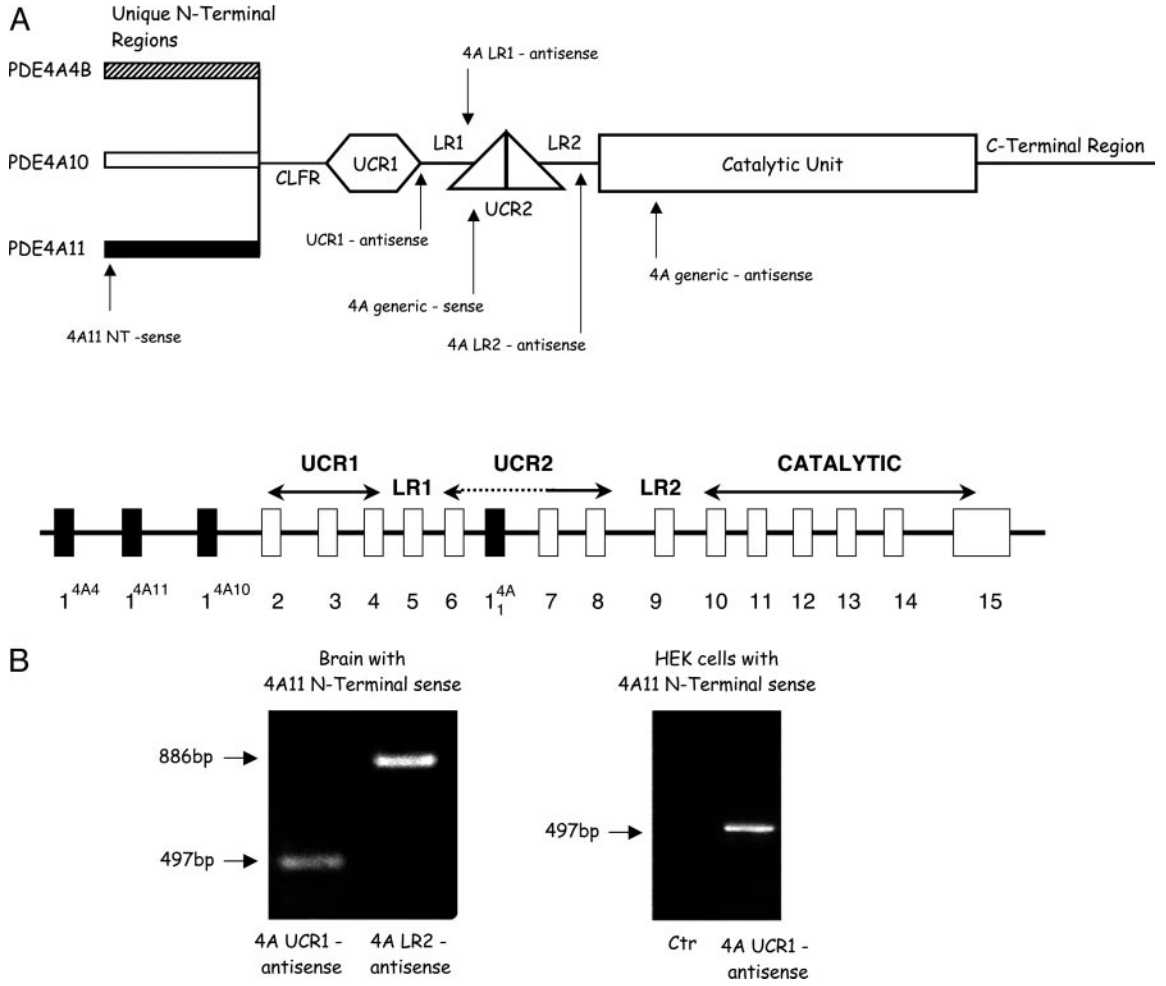

Fig. 3. PDE4A11 is a long isoform encoded by the PDE4A gene. A, top, a schematic of the key regions of PDE4A11 as inferred from EST analysis and by reference to the structure of established PDE4 long isoforms. Shown schematically are the N-terminal regions unique to the three long PDE4A isoforms, namely PDE4A4B (GenBank accession number L20965), PDE4A10 (GenBank accession number AF110461), and PDE4A11 (GenBank accession number AY618547). Also indicated are the positions of primers used in RT-PCR studies, for which sequence details are given under *Materials and Methods*. UCR, upstream conserved region; LR, linker region; CLFR, common long form region, as described in Houslay (2001). Assuming ATG = 123 in the 4A11 ORF, then 4A11 NT sense RT-PCR probe is nucleotides 1 to 25; 4A11 UCR1 antisense RT-PCR probe is nucleotides 471 to 497; 4A11 LR2 antisense RT-PCR probe is nucleotides 859 to 886; 4A11 expression profile sense probe is nucleotides 33 to 50; and 4A11 expression profile antisense probe is nucleotides 507 to 527. Prove sequences are described under *Materials and Methods*. Bottom, the coding exons (boxes) for active PDE4A isoforms, with the unique 5′ exons shown as ■, are shown schematically. PDe4A1 is a supershort isoform that lacks UCR1 and has a truncated UCR2, whereas PDE4A4B, PDE4A10, and PDE4A11 are long isoforms. B, left, RT-PCR analysis done on human brain mRNA with a sense primer targeted within the unique region of PDE4A11 and an antisense primer targeted within either UCR1 or LR2, as indicated. Right, RT-PCR analysis done on HEK293 cells with a sense primer targeted within the unique region of PDE4A11 and an antisense primer targeted within UCR1.

We also compared transcript levels for PDE4A11 relative to those for the PDE4A10 and PDE4A4B long isoforms in various human blood cell types (Fig. 4B). These data clearly show that PDE4A11 is widely expressed and, indeed, transcripts for it seem to provide the major species in a variety of cells, including monocytes, mast cells, and macrophages, as well as in bronchial smooth muscle. On the other hand, PDE4A4B seems to provide the major level of transcripts in T cells (Fig. 4B).

Promoter Activity of the 5′ Region of PDE4A11. The 1-kb region immediately 5′ of the ATG start in human exon-1^{4A11} was cloned into the vector pGL to evaluate any potential promoter activity by assessing the luciferase reporter function. This reporter construct was transfected into HEK293 cells, whereupon a marked increase in luciferase activity was evident over that seen upon transfection of the base plasmid pGL3-basic (Fig. 5a). Alongside this, we compared the activity of the PDE4A10 promoter construct, which we have described previously (Rena et al., 2001), and the putative PDE4A4B promoter construct, which in all instances was similarly formed from 1 kb of intronic sequence located immediately 5′ to the ATG start site within exon-1^{4A10} and exon-1^{4A4B}, respectively (Fig. 5a). It is interesting that both the PDE4A11 and PDE4A10 promoter constructs gave similarly high activities in these cells, with less activity seen with the PDE4A4B construct (Fig. 5a). These data indicate that there is a functional promoter immediately upstream of the ATG start site in exon-1^{4A11}.

We then generated a panel of 5′ deletion constructs of the PDE4A11 reporter construct and assessed their activity in HEK cells (Fig. 5b). Deletion of either 250 or 500 bp to yield the "750-bp" and "500-bp" reporter constructs, led to little or no change in luciferase activity (Fig. 5b). It is interesting that deletion to yield the "250-bp" construct led to a doubling of activity over that seen with the 500-bp construct (Fig. 5b), implying that some repressor element may be functioning in

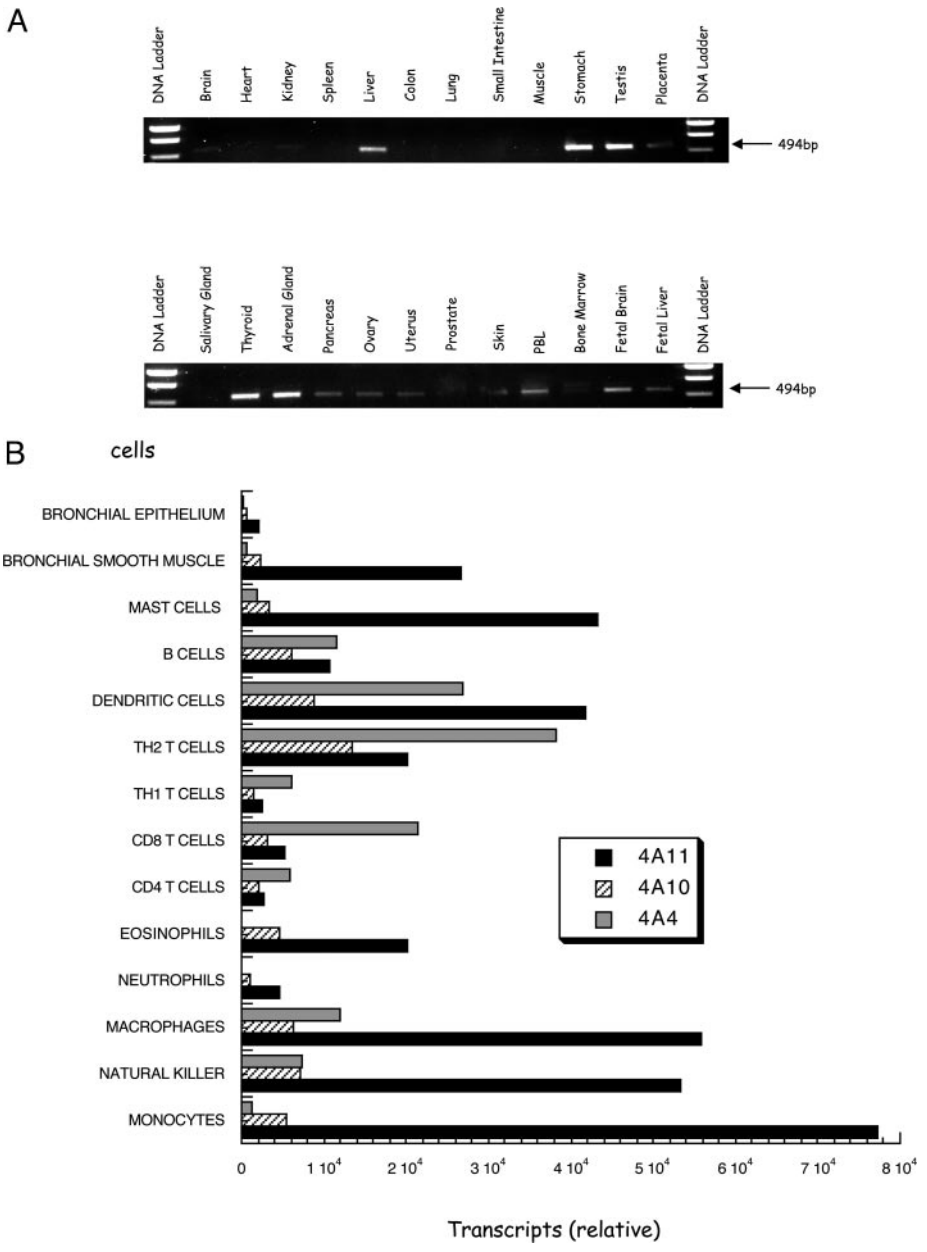

Fig. 4. Expression profile of PDE4A11. A, RT-PCR analysis of the distribution of transcripts for PDE4A11 as identified in a panel of human RNA probed by RT-PCR using a sense primer targeted within the unique region of PDE4A11 and an antisense primer targeted within LR1. The data shown are representative of an experiment done three times. B, TaqMan mRNA profiles assessing the distribution of transcripts for PDE4A4B, PDE4A10, and PDE4A11 in various human blood cell types as well as bronchial epithelium and bronchial smooth muscle. These data are from cells pooled from three normal individuals.

the 250- to 500-bp region. These data indicate that the first 250 bp found immediately 5′ to the ATG start site in exon-1^{4A11} contains elements that suffice to allow for promoter activity that we would expect to drive basal transcription of PDE4A11. Although this region does not contain a classic TATA box it is within a CpG-rich island (Fig. 1B) and exhibits, as do a number of TATA-less promoters, a number of consensus sites for binding of the SP1 transcription factor, some of which are conserved between human and mouse (Fig. 5c).

Expression of Recombinant PDE4A11 in COS-7 Cells. An expression construct of the entire ORF for PDE4A11, encoding 860 amino acids, was generated in pcDNA3. This was used for transient expression studies in mammalian COS-7 cells. COS-7 cells transfected to express PDE4A11 exhibited a cAMP PDE activity of 4 to 6 nmol/min/mg protein, compared with the 4 to 6 pmol/min/mg protein seen in nontransfected cells (range, $n = 3$). Assayed using 1 μM cAMP as substrate, more than 98% of the cAMP PDE activity in these cells was inhibited by the archetypal PDE4 selective inhibitor rolipram (10 μM). Thus, recombinant PDE4A11 expressed in these cells shows the properties expected of a PDE4 family member and provides the major cAMP PDE activity in these transfected cells.

Immunoblotting (Fig. 6a) of PDE4A11-transfected cells with a "pan-PDE4A"–specific antiserum generated against the C-terminal region found in common to all PDE4A isoforms identifies the presence of a single immunoreactive species of 126 ± 4 kDa (mean ± S.D.; $n = 3$). The size of PDE4A11 on SDS-PAGE is comparable with that observed for the other two known PDE4A4 long isoforms, namely PDE4A4B (125 kDa) and PDE4A10 (121 kDa). Thus, in endogenous expression systems, these three long isoforms will not be readily distinguished by Western blotting using pan-4A–specific antisera. However, all are considerably larger than that of the 83-kDa PDE4A1 short isoform, and all migrate on SDS-PAGE with substantially greater molecular masses than predicted by their primary amino acid sequence (Rena et al., 2001). Thus, the predicted size of PDE4A11 is some 95.3 kDa, which is approximately 30 kDa less than that observed in SDS-PAGE. Deletion studies have shown that this aberrant migration is caused by a region located within the conserved PDE4A catalytic core (Johnston et al., 2004).

Subcellular fractionation studies showed that some 52 ± 2% (mean ± S.D.; $n = 3$) of PDE4A11 was located within the S2, high-speed supernatant fraction, with the rest being particulate-associated. Immunohistochemical analysis using confocal microscopy (Fig. 6b) of COS-7 cells transfected to express PDE4A11 showed that it was excluded from the nucleus and concentrated in the perinuclear region and at the cell margin.

We have demonstrated that long-term challenge of HEK, Chinese hamster ovary, and rat basophilic leukemia cells expressing recombinant PDE4A4B caused a profound redistribution of PDE4A4B into foci within the cytoplasm (Terry et al., 2003). This reversible process is cAMP-independent

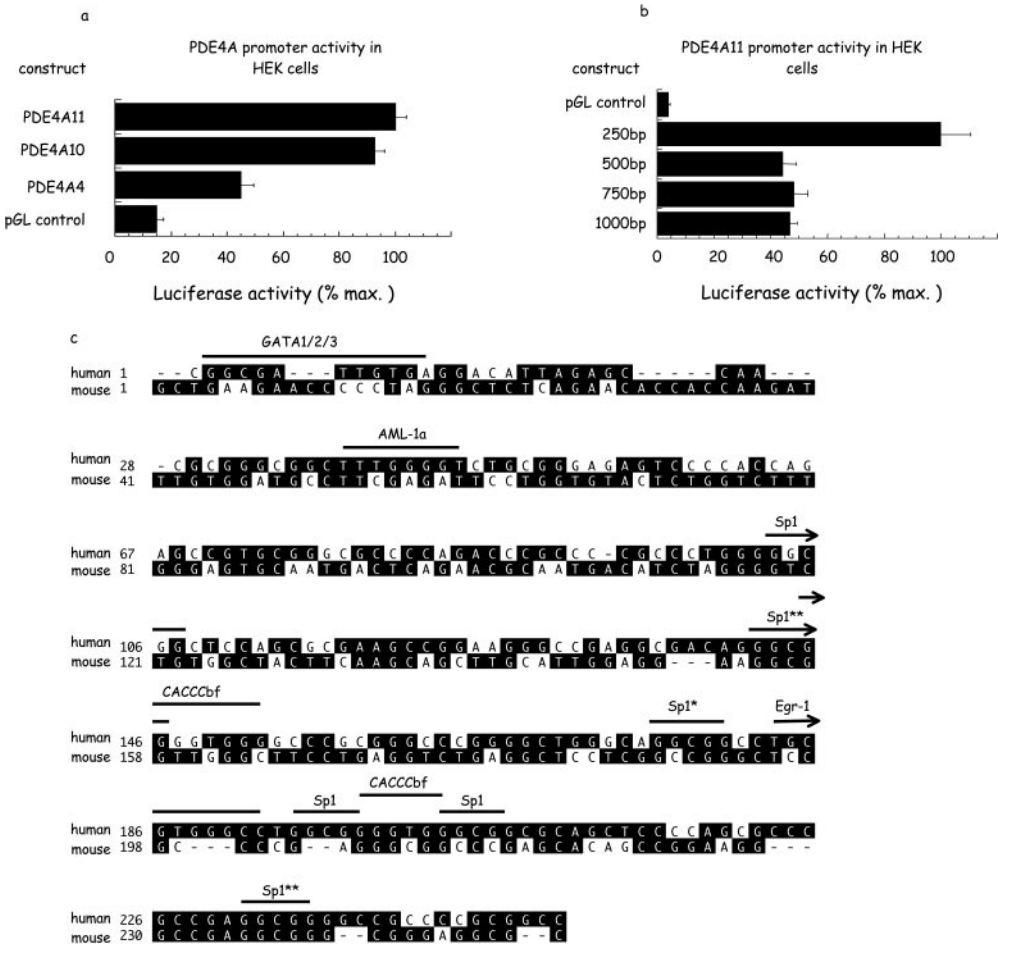

Fig. 5. Promoter activity associated with the intron upstream of the unique PDE4A11 5′ exon. a, results of luciferase reporter assays for three putative promoter evaluation constructs. These were formed by cloning 1-kb regions located immediately 5′ of each of the human exon-1^{4A4b}, exon-1^{4A10}, and exon-1^{4A11} into the vector pGL. These were then transfected into HEK293 cells to evaluate any potential promoter activity of these constructs by assessing luciferase activity. Data are shown as relative percentage to that observed with the PDE4A11 construct (100%) for $n = 5$ separate transfections (means ± S.D.). b, luciferase reporter assay for various 5′ truncates of the 1-kb putative PDE4A11 promoter construct (as above) transfected into HEK293 cells with data are shown as relative percentage to the maximal activity observed (100%), in this case with the construct formed from 250 bp immediately upstream of the unique PDE4A11 exon (data are means ± S.D. for $n = 4$ separate transfections). c, comparison of the 250 bp of intronic sequence found immediately upstream of the ATG start site for PDE4A11 in both human and mouse. Examples of putative transcription binding sites are indicated. Sp1** are completely conserved in human and mouse, Sp1* are highly conserved in human and mouse, and Sp1 are unique to human. ■, conserved sequence.

and is presumed to be triggered as a consequence of a conformational change induced through the binding of the selective, competitive inhibitor rolipram to the active site of PDE4A4B. Such a profound redistribution was observed using wild-type PDE4A4, as well as chimeras formed with various tags, including GFP, which allows for visualization in living cells. Here we see in living COS cells that treatment with rolipram induced foci formation of GFP-tagged PDE4A4B (Fig. 6c). In marked contrast to this, however, rolipram treatment did not cause GFP-tagged versions of either PDE4A11 or PDE4A10 to form foci in these cells (Fig. 6c). As observed with untagged PDE4A11 (Fig. 6b), GFP-tagged PDE4A11 in COS cells was concentrated in the perinuclear region and also was observed within ruffles at the cell margin (Fig. 6c). We noted that unlike PDE4A11, neither PDE4A4 nor PDE4A10 was found within ruffles, highlighting this as a unique facet of the intracellular localization of PDE4A11 (Fig. 6c).

Analysis of cAMP hydrolysis of soluble PDE4A11 showed it to have a K_m value of 4.2 ± 1.1 μM and that of the particulate activity a K_m of 3.7 ± 1.8 μM (mean ± S.D.; n = 3). Such values are very similar to those exhibited by other PDE4 isoforms, including the PDE4A4B and PDE4A10 long isoforms (Huston et al., 1996; Rena et al., 2001). We then set out to evaluate how actively PDE4A11 hydrolyzed cAMP compared with the other long PDE4A isoforms. To do this, we took equal immunoreactive amounts of soluble PDE4A11 and PDE4A4B to determine a "relative V_{max}" value. This yielded a ratio of 1.1 ± 0.1 (mean ± S.D.; n = 3) for the activity of PDE4A11 compared with PDE4A4B. From these data and those reported previously by us (Rena et al., 2001), the ratio of V_{max} values for long PDE4A isoforms was (1):1:1.1 for PDE4A4B/PDE4A10/PDE4A11. Thus, all long PDE4A isoforms seem to be similarly active. We also noted that particulate association of PDE4A11 had little effect on its maximal catalytic activity, with the ratio of the V_{max} value for total particulate to soluble PDE4A11 being some 1.1 ± 0.1 (mean ± S.D.; n = 3).

Rolipram is the archetypal selective PDE4 inhibitor (Houslay and Adams, 2003). It dose-dependently inhibits cytosolic PDE4A11 activity with an IC_{50} value of 0.72 ± 0.08 μM (mean ± S.D.; n = 3) (Fig. 7 and Table 2). This is comparable with values of 0.056 and 1.25 μM for the soluble forms of PDE4A10 and PDE4A4B, respectively (Huston et al., 1996; Houslay, 2001; Rena et al., 2001).

PDE4A11 is also dose-dependently inhibited by a variety of other PDE4-selective inhibitors, namely Ro 20-1724, cilomilast (Ariflo; GlaxoSmithKline), roflumilast, and denbufylline

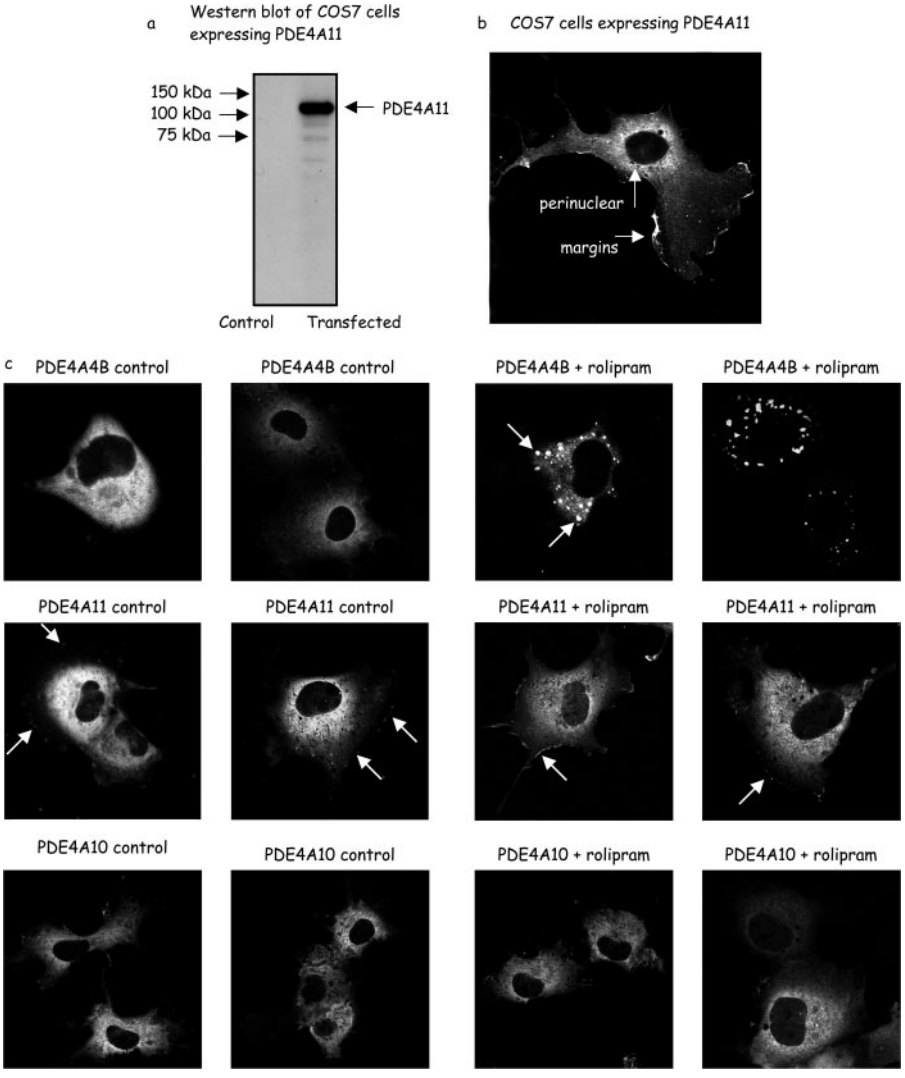

Fig. 6. Expression of recombinant PDE4A11 in COS-7 cells. a, Western blot of lysates from COS-7 cells that either had (Tr) or had not (Ctr) been transfected with a plasmid encoding PDE4A11. In the transfected cells, a single 126-kDa immunoreactive species was identified using a "pan-PDE4A" antiserum able to detect all active human PDE4A isoforms. b, a confocal section through a fixed COS-7 cell transfected to express wild-type PDE4A11 and visualized immunologically using a human PDE4A-specific antiserum. Note that fluorescence is focused toward the perinuclear region of the cell with centers of fluorescence located at the cell margin, as indicated by the white arrows. At similar gain, no fluorescence was evident in cells that had either not been transfected or transfected with empty vector. c, shown are confocal sections through living COS cells transfected to express C-terminal GFP-tagged forms of PDE4A4B, PDE4A11, and PDE4A10, as indicated. Additionally shown are such cells that had been incubated for 16 h with rolipram (10 μM). In the section showing rolipram-treated cells expressing PDE4A4B, the white arrows indicate examples of foci. In the sections showing untreated cells expressing PDE4A11, the white arrows indicate examples of PDE4A11 located within ruffles at the cell margins. These data are typical of experiments done at least three times with different transfections.

(Fig. 8 and Table 1). IC_{50} values range from approximately 1 μM for Ro 20-1724 down to approximately 4 nM with roflumilast (Table 2). However, in each instance, we noted that there was no difference in sensitivity of the cytosol and particulate forms of PDE4A11 to any particular inhibitor (Table 2). We also determined the sensitivity of PDE4A4 and PDE4A10 to inhibition by these various compounds (Table 2). In doing so, we noted that PDE4A10 is considerably less sensitive to inhibition by Ariflo, albeit considerably more sensitive to inhibition by rolipram, than either of the other two long isoforms (Table 2). Indeed, PDE4A11 seems to be slightly more sensitive to inhibition by Ariflo and denbufylline than either of the other two isoforms (Table 2). PDE4A4 seems to be slightly less sensitive to inhibition by Ro 20-1724 than either of the other two long PDE4A isoforms (Table 2). We also see here that as for rolipram, particulate PDE4A4 is more sensitive to inhibition by roflumilast compared with its soluble form (Table 2).

The denaturation of enzyme proteins by heat occurs as a first-order process that can be followed by analysis of the exponential decay in their catalytic activity. A semilog plot of the log% activity remaining against time thus allows for a determination of the half-life of inactivation ($t_{1/2}$). Here we see that incubation at 55°C causes the inactivation of both soluble and particulate PDE4A11 as a single exponential (Fig. 8). However, in each of these instances there is a marked difference with $t_{1/2}$ values of 2.5 ± 0.3 min for soluble PDE4A11 (S2 fraction) and 4.4 ± 0.3 min for particulate PDE4A11 (mean ± S.D.; n = 3 separate experiments).

Phosphorylation of PDE4A11 by PKA. Various long PDE4 isoforms can be activated through phosphorylation by PKA, which occurs at a consensus site (RRESF) for phosphorylation located in the PDE4 UCR1 regulatory module (Sette and Conti, 1996; Hoffmann et al., 1998; MacKenzie et al., 2002). Phosphorylation of this site by PKA can readily be monitored using an antiserum specific for the phosphorylated form of UCR1 (MacKenzie et al., 2002). Here, we see that treatment of COS-7 cells transfected to express PDE4A11 with the adenylyl cyclase activator forskolin (100 μM) together with the nonselective PDE inhibitor IBMX (100 μM) to raise intracellular cAMP levels (MacKenzie et al., 2002) leads to the phosphorylation of PDE4A11, as indicated by the detection of a 126-kDa immunoreactive species with the P-UCR1 antiserum (Fig. 9a). The appearance of this 126-kDa immunoreactive species occurs in a time-dependent fashion after the addition of forskolin and IBMX (Fig. 9a) to COS-7 cells and is not evident in nontransfected cells analyzed under comparable levels of exposure in the ECL detection system (data not shown). The appearance of this immunoreactive species in cells challenged with forskolin together with IBMX is ablated in a dose-dependent fashion when the PKA-selective inhibitor H89 is also present (Fig. 9b). When cells transfected to express the Ser119Ala-PDE4A11 construct, in which the target serine for phosphorylation by PKA in UCR1 has been mutated to alanine, are challenged with forskolin together with IBMX, then no immunoreactive species is detected with the P-UCR1 antiserum (Fig. 9c).

Treatment of COS-7 cells expressing PDE4A11 with forskolin (100 μM) together with IBMX (100 μM) leads to the activation of PDE4A11 in a time-dependent fashion (Fig. 9d), which reflects that seen for its phosphorylation (Fig. 9e). In contrast to this, challenge of COS-7 cells expressing the

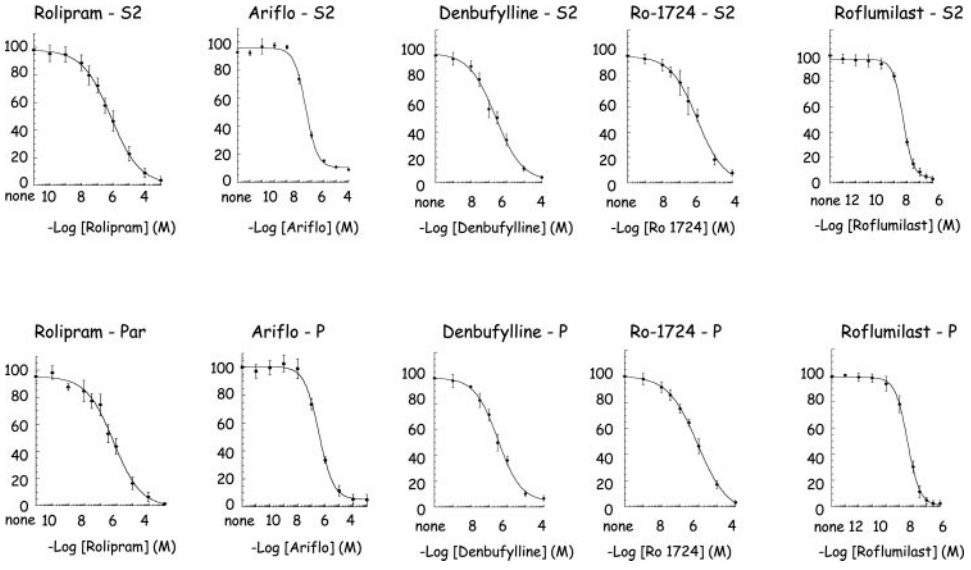

Fig. 7. Inhibition of PDE4A11 by selective PDE4 inhibitors. cAMP PDE activity assays on PDE4A11 were performed using 1 μM cAMP as substrate with the range of inhibitor concentrations and type of inhibitor, as indicated in each graph. The structures of the various inhibitors used in this study are provided as Supplemental Fig. S1. Analyses were done on both soluble (S2) fraction PDE4A11 and particulate (P1 + P2)-associated PDE4A11. The data are averages for three separate experiment shown as means ± S.D.

TABLE 2
Inhibition of PDE4A11 by PDE4 family-selective inhibitors
Assays were done with 1 μ M cAMP as substrate using the range and number of inhibitor concentrations as indicated in Fig 8. By far the major fraction of PDE4A10 is soluble in lysed cells, and thus data are only provided for the S2 fraction. The data reflect the average of three separate experiments with IC_{50} values given as the mean ± S.D. in micromoloar concentrations.

Inhibitor	PDE4A11 (S2)	PDE4A11 (P2)	PDE4A4B (S2)	PDE4A4B (P2)	PDE4A10 (S2)
Rolipram	0.72 ± 0.08	0.66 ± 0.12	1.31 ± 0.08	0.26 ± 0.09	0.064 ± 0.009
Ariflo (cilomilast)	0.034 ± 0.005	0.034 ± 0.005	0.061 ± 0.007	0.059 ± 0.004	0.13 ± 0.03
Roflumilast	0.0048 ± 0.0004	0.0039 ± 0.0002	0.0090 ± 0.0016	0.0025 ± 0.0009	0.0041 ± 0.0008
Denbufylline	0.25 ± 0.06	0.31 ± 0.04	0.56 ± 0.30	0.46 ± 0.20	0.59 ± 0.17
Ro 20-1724	0.99 ± 0.11	0.91 ± 0.07	2.93 ± 1.16	2.90 ± 0.10	1.24 ± 0.07

Ser119Ala-PDE4A11 construct with forskolin (100 μM) together with IBMX (100 μM) did not lead to any change (<7%; n = 3 experiments) in cAMP PDE activity. Likewise, no change in cAMP PDE activity (<6%) occurred in COS-7 cells expressing PDE4A11 that were challenged with forskolin (100 μM) together with IBMX (100 μM) in the presence of the PKA inhibitor H89.

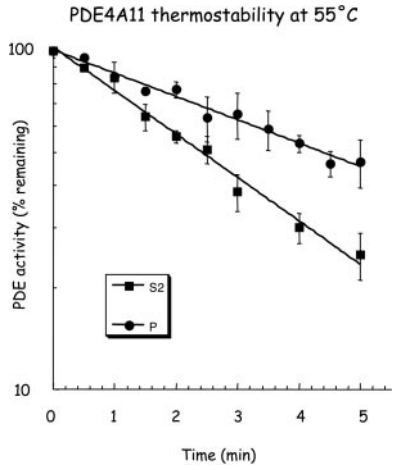

Fig. 8. Thermostability of PDE4A11. Soluble (S2) and particulate (P) fractions of PDE4A11 were incubated for the indicated times at 55°C before assay of their cAMP PDE activity with 1 μM cAMP as substrate. The log% residual activity is plotted here as a function of time, with the half-life determined as that time in which 50% of the activity remained. Data are from three separate experiments with means ± S.D. are shown.

Interaction of PDE4A11 with the SH3 Domain of LYN. Pull-down (sedimentation) assays have been used to show that the SH3 domain of LYN tyrosyl kinase, expressed as a GST fusion protein, binds to the long PDE4A4 isoform (McPhee et al., 1999; Rena et al., 2001). Deletion analyses then showed that the unique N terminus of PDE4A4 provided the major site of interaction, with the LR2 segment found in all active PDE4A isoforms providing another site of interaction (McPhee et al., 1999). Here we show that although PDE4A11 is able to interact with the SH3 domain of LYN, the magnitude of such an interaction is less than that observed with PDE4A4 (Fig. 10a). Indeed, the degree of interaction is apparently similar to that seen using PDE4A10 (Fig. 10a).

Action of Caspase-3. The rodent PDE4A5 isoform has been shown to provide a substrate for caspase-3 action (Huston et al., 2000). This cleaves at a single site within a caspase-3 consensus sequence (DAVD) located in the unique N-terminal region of PDE4A4. We see here that activated caspase-3 also acts on the 127-kDa PDE4A4 isoform, which is the human homolog of PDE4A5, to yield a 120-kDa species

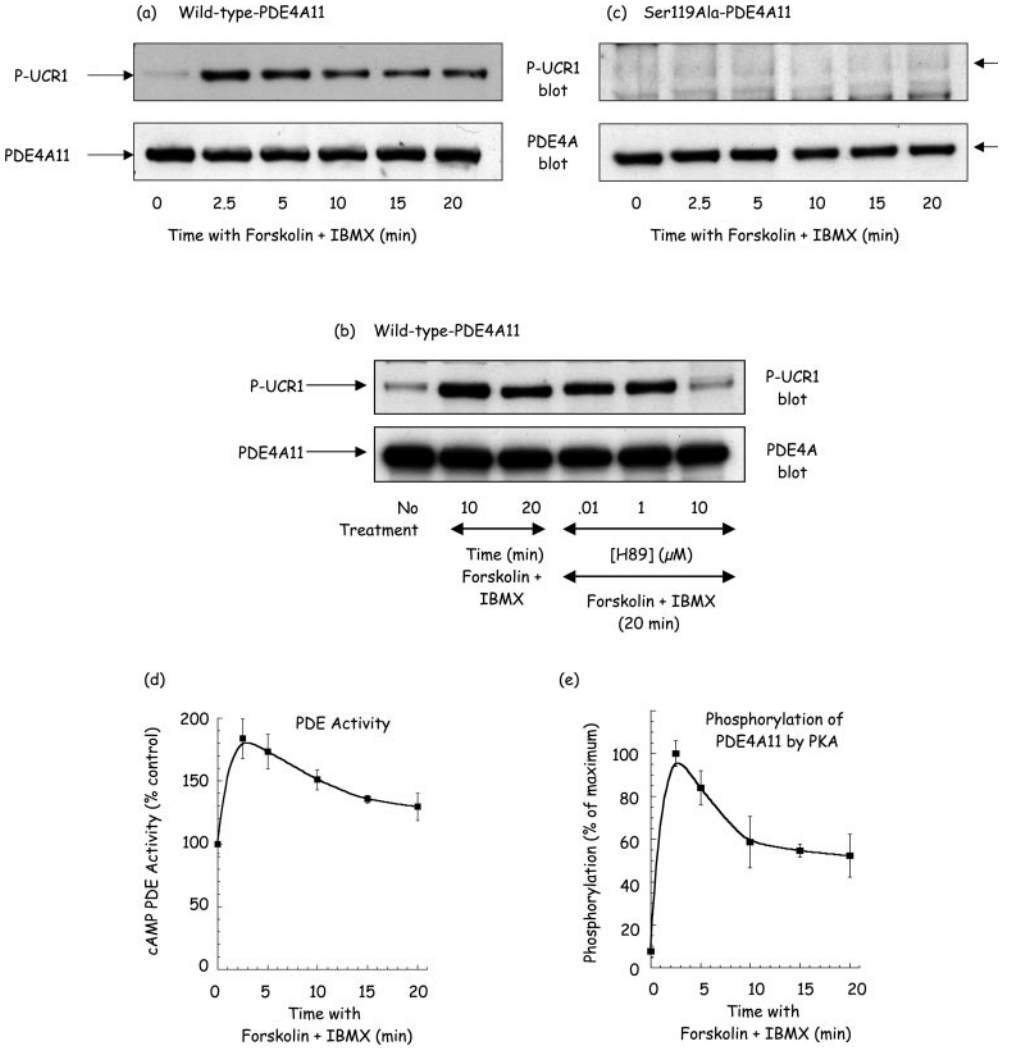

Fig. 9. PDE4A11 is phosphorylated by PKA. a, COS-7 cells transfected to express PDE4A11 are challenged with forskolin (100 μM) together with IBMX (100 μM). At the indicated times, cells were harvested, and lysates were analyzed by Western blotting using an antisera specific for the phosphorylated form of UCR1, within the motif RRES(Phospho)W. A 126-kDa single immunoreactive band was identified in a time-dependent fashion (top). Bottom, the result of Western blotting these fractions with a pan-PDE4A antiserum so as to provide loading controls. b, dose-dependent inhibitory effect that the PKA inhibitor H89 exerts on this process, with blotting in the top showing data for the phospho-UCR1 antiserum with an arrow indicating the expected position for PDE4A11 and the bottom providing the loading control done with a PDE4A antiserum. c, effect of treating cells transfected with the S119A mutant form of PDE4A11 with forskolin (100 μM) together with IBMX (100 μM) for the indicated times before immunoblotting as described above with these two antisera. d, effect of treating COS-7 cells transfected to express PDE4A11 for the indicated times with forskolin (100 μM) together with IBMX (100 μM) on the lysate PDE4A11 activity for three separate experiments with data as means ± S.D. e, the densitometric quantification of the labeling of P-UCR1 in COS-7 cells transfected to express PDE4A11 and challenged with forskolin (100 μM) together with IBMX (100 μM) with lysates analyzed at the indicated times cells (as in Fig. 10a) but for three separate experiments with data as means ± S.D.

(Fig. 10b). This faster migrating, cleaved species is detected with the PDE4A C-terminal antibody. However, consistent with cleavage occurring in the unique N-terminal region of PDE4A4, such a faster migrating species is not seen using the PDE4A4-specific antiserum, which is targeted to the cleaved extreme N-terminal portion of PDE4A4 (Fig. 10b). However, it is apparent that the intensity of the signal detected by this PDE4A4-specific N-terminal antiserum is reduced in the caspase-3–treated track, consistent with a diminished amount of full-length species caused by caspase-3 action (Fig. 10b). The presumed site of cleavage in PDE4A4 by caspase-3 is the cognate one (D^{69}AMD) to that in PDE4D5 (D^{69}AVD), which would remove a ~7-kDa fragment, consistent with the observed mobility shift (Fig. 10b). In contrast to this, caspase-3 failed to cause any change in either the mobility of PDE4A11 and PDE4A10 or the intensity of the single immunoreactive species detected with the PDE4A C-terminal antibody (Fig. 10). This is consistent with there not being any caspase-3 consensus motif within the unique N-terminal regions of either of these two species.

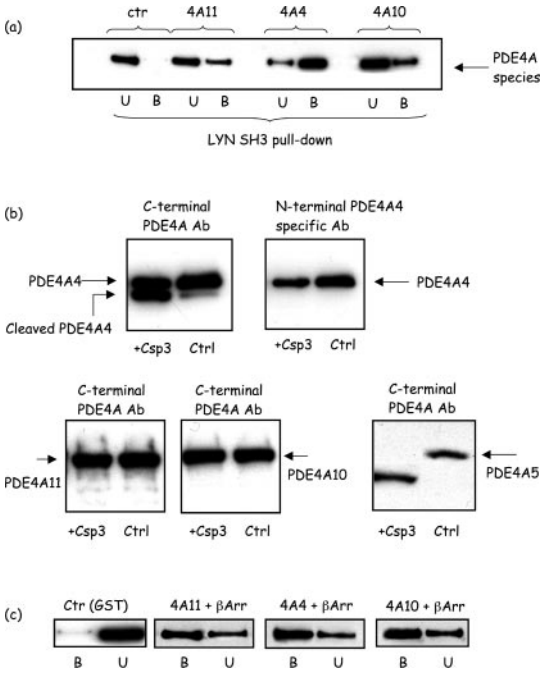

Fig. 10. Evaluation of LYN SH3, caspase-3 and β-arrestin2 on PDE4A11. a, pull-down assays to probe the interaction between the indicated PDE4A isoforms and the purified SH3 domain of LYN expressed as a GST fusion protein. B, the GST-(LYN SH3 domain) fraction bound to glutathione agarose beads; U, the unbound fraction from the pull-down experiment. This analysis was done exactly as we described previously for PDE4A11 and PDE4A4 (McPhee et al., 1999; Rena et al., 2001), with equal levels of input of each PDE4A species, as assessed immunologically using the C-terminal PDE4A-specific antiserum. Thus, the level of pull-down achieved by GST-LYN SH3 can be compared for the indicated three long PDE4A isoforms, with visualization done using the PDE4A-specific antiserum in Western blots. The control is a bead pull-down done using GST alone and with PDE4A11 present; similar null pull-down was achieved with PDE4A4 and PDE4A10 in the presence of GST as described previously (McPhee et al., 1999; Rena et al., 2001). b, the effect of incubating the indicated PDE4A long isoform with activated caspase-3. Equal immunoreactive amounts of the indicated PDE4A isoforms were incubated with the same amount of activated caspase-3 (see *Materials and Methods*) before analysis by Western blotting with an antibody directed to the common C-terminal region of PDE4A. Shown are the only immunoreactive species apparent, and the gels are typical of ones done at least three times. PDE4A10 and PDE4A11 were identified as single bands whose migration and intensity were unaffected by caspase-3 treatment (approximately 126 kDa). Untreated PDE4A4 migrated at 127 kDa; however, caspase-3 treatment caused the appearance of a novel 120-kDa species detected by the pan-PDE4A (C-terminal) antisera but which was not seen with the PDE4A4-specific (N-terminal) antiserum. Also shown is the action of caspase-3 on the rodent PDE4A4 homolog PDE4A5. c, pull-down assays to probe the interaction between the indicated PDE4A isoforms and the purified GST fusion protein of β-arrestin as described before (Perry et al., 2002; Baillie et al., 2003; Bolger et al., 2003). Descriptions are as in "a" above. All of these data are typical of experiments done three times with different transfections.

Interaction of PDE4A11 with β-arrestin2. β-arrestin seemingly has the potential to interact with PDE4 enzymes from all subfamilies (Perry et al., 2002), which is presumed to result from a common binding site in the conserved PDE4 catalytic unit (Bolger et al., 2003). Given that the catalytic unit of PDE4 isoforms within a subfamily may be affected by the N-terminal region, as indicated by different thermostability and inhibitor sensitivities, we set out to determine whether these three PDE4 isoforms could potentially interact with β-arrestin. As done before by us for PDE4D, we used a pull-down assay with β-arrestin-GST and the various PDE4A isoforms expressed in *E. coli*. Using equal immunoreactive mounts of each of these three isoforms, we see here that all three species can interact with β-arrestin (Fig. 10c).

Discussion

PDE4 isoforms provide targets for novel anti-inflammatory therapeutics (Burnouf and Pruniaux, 2002; Giembycz, 2002) and serve to determine compartmentalized cAMP signaling (Mongillo et al., 2004). Here we have identified a novel human PDE4A long isoform, called PDE4A11, that is highly conserved among species (Fig. 2). Available sequence for the unique portion of PDE4A11 (Fig. 2A) indicates that although pig and bat sequences show 90% identity with human PDE4A11, this decreases to 54% in rodents, suggesting caution in extrapolating data from rodent studies to human.

Transcript analysis (Fig. 4) indicates that PDE4A11 is widely expressed in human tissues, including cells involved in inflammatory responses. Indeed, PDE4A11 transcript levels are invariably similar to or even greater than those of the two other known PDE4A long isoforms, PDE4A4B (Bolger et al., 1993) and PDE4A10 (Rena et al., 2001). Although attention thus far has focused on PDE4A4B, levels of PDE4A4B transcripts seem to be in lowest abundance (Fig. 4). If possible, we would have liked to undertake immunological analyses. However, we have been unsuccessful in trying to generate PDE4A11-specific antisera.

We have identified a functional promoter for PDE4A11, with basal activity contained within a 250-bp region located immediately 3′ to the ATG start site for PDE4A11 (Fig. 5). As with all PDE4 isoform promoters identified to date (Vicini and Conti, 1997; Rena et al., 2001; Le Jeune et al., 2002), this region contains a series of perfect stimulating protein 1 (Sp1) consensus binding sites. Such sites typically drive basal transcription of genes that like those for PDE4 isoforms lack a canonical TATA box and reside in CpG-rich islands. In this 250-bp region, there are potential binding sites for early growth response-1, GATA-1/2/3, and AML-1a transcription factors, which have been shown to synergize with Sp1 in driving basal promoter activity of various genes (Alfonso-Jaume et al., 2004). Two of the putative Sp1 sites have overlapping CACCC binding-factor sites, a situation that in

the monoamine oxidase B gene confers inhibitory regulation (Ou et al., 2004).

PDE4A long isoforms differ from each other by their unique N-terminal regions, which are encoded by distinct 5′ exons (Sullivan et al., 1998; Houslay and Adams, 2003). In the case of PDE4A11, exon1^{4A11} encodes a region of 81 amino acids that bears no similarity to that of any other known PDE4 isoform. The core PDE4A species is an entirely cytosolic entity (Sullivan et al., 1998), indicating that the N-terminal region of PDE4A11, like that of other PDE4 isoforms (Huston et al., 1996; McPhee et al., 1999; Rena et al., 2001; Baillie et al., 2002), has a role in intracellular targeting. Here we see that PDE4A11 is primarily localized to the perinuclear region but is also found in ruffles at the cell plasma membrane, as shown for the wild-type PDE4A11 in fixed cells and for GFP chimera in living cells (Fig. 6). Cell disruption identifies a soluble component, although it is unclear as to whether this reflects cytosolic PDE4A11 or PDE4A11 that reversibly and weakly binds to particulate anchor proteins and is released upon cell breakage.

As reported previously (Terry et al., 2003), long-term treatment of COS cells with rolipram causes a profound change in the intracellular distribution of PDE4A4B, namely its reversible relocalization to foci within cells (Fig. 6c). Such a reorganization is induced by a conformational change in PDE4A4B, occurring upon rolipram binding (Terry et al., 2003). This is specific to PDE4A4 rather than generic for PDE4A long isoforms, because neither PDE4A11 nor PDE4A10 shows any such redistribution. Indeed, PDE4A4B (McPhee et al., 1999) but neither PDE4A11 nor PDE4A10 (Table 2) exhibits a dramatic increase in affinity for rolipram upon membrane binding. This identifies PDE4A4B alone as being peculiarly sensitive to conformational changes involving rolipram.

Thermal denaturation analyses provide a simple means of evaluating differences in the conformational status of closely related proteins. We have shown (Rena et al., 2001) that although incubation at 55°C causes the inactivation of PDE4A4B and PDE4A10 to occur as single exponentials, this is characterized by very different half-lives. Thus, cytosolic PDE4A4B is more thermostable ($t_{1/2}$ = 22 min) than PDE4A10 ($t_{1/2}$ = 11 min). Here we see that PDE4A11 is different again, with the cytosolic enzyme being dramatically more labile, decaying with $t_{1/2}$ of 2.5 min (Fig. 8). The unique N-terminal region of each of these isoforms seems to exert a distinct effect on the conformational status of the PDE4A catalytic unit. The functional significance of this remains to be ascertained, although, clearly, it does not translate into any change in catalytic activity because the K_m values and relative V_{max} values of these isoforms are nearly identical. It is interesting, however, that whereas particulate PDE4A11 is more thermostable ($t_{1/2}$ = 4.4 min) than its cytosolic component (Fig. 8), the converse is true for both PDE4A10 ($t_{1/2}$ = 5 min) and PDE4A4B ($t_{1/2}$ = 12.5 min) (Rena et al., 2001). Because the N-terminal regions of PDE4 isoforms have an important role in intracellular targeting (Conti et al., 2003; Houslay and Adams, 2003), our data suggest that particulate association exerts distinct effects on the conformational status of each of these isoforms. Indeed, the N-terminal domain together with LR2 allows PDE4A4 to interact with the SH3 domains of SRC family tyrosyl kinases, particularly LYN (McPhee et al., 1999). The N-terminal interaction affects intracellular targeting (Beard et al., 2002), although the combined interaction at these two sites affects the conformation of the catalytic unit of PDE4A4 (McPhee et al., 1999). PDE4A11 and PDE4A10 lack consensus sites for SH3 domain interaction in their unique N-terminal regions; thus, interaction is confined to the common LR2 region, explaining their reduced interaction compared with PDE4A4 with the SH3 domain of LYN (Fig. 10a). Differences in interaction with proteins may contribute to altered conformations of these isoforms, with changed functional attributes and altered thermostability. In this regard, β-arrestins, which act as a multifunctional scaffold protein responsible for desensitizing G-protein–coupled receptors (Perry and Lefkowitz, 2002), have recently been shown to bind PDE4 enzymes, thereby recruiting active PDEs to the site of cAMP synthesis in cells (Perry et al., 2002). We show here that all three PDE4A long isoforms have the potential to interact with β-arrestin2 (Fig. 10c). This is consistent with the notion that

TABLE 3
Summary of PDE4A11 distinguishing features

Property	Comment
Rolipram inhibition	Unlike 4A4, particulate and soluble forms of 4A11 show no difference in sensitivity to inhibition by rolipram
Long-term rolipram treatment	Unlike 4A4, chronic treatment of cells with rolipram does not cause redistribution of 4A11 within cells
Ro 20–1724	4A11 and 4A10 are more potently inhibited than 4A4
Roflumilast	Unlike 4A4, soluble and particulate 4A11 forms show similar sensitivity to inhibition by roflumilast
Denbufylline	4A11 is more sensitive to inhibition than 4A4 or 4A10
Ariflo (cilomilast)	4A10 is less sensitive to inhibition than 4A4 or 4A11
Distribution	Unlike 4A4 and 4A11, 4A11 is found in plasma membrane ruffles
LYN (SH3 domain)	4A11 and 4A10 show a lower propensity of associating with LYN through its SH3 domain than does 4A4
Thermal stability of soluble 4A11	Soluble 4A11 is dramatically more thermolabile than the soluble form of other PDE4A long isoforms
Thermal stability of particulate 4A11	Particulate 4A11 is more thermolabile than 4A4 but similarly thermolabile to 4A10
Comparative thermostability of soluble and particulate forms	Although particulate 4A11 is more thermostable than cytosolic 4A11, the converse is true for both 4A10 and 4A4
Caspase-3	Only PDE4A4 is cleaved by caspase-3
β−arrestin2	All three isoforms can interact with β−arrestin2
PKA phosphorylation	Similar to other PDE4A long isoforms
K_m cAMP	Similar to other PDE4A long isoforms
V_{max} cAMP hydrolysis	Similar to other PDE4A long isoforms

β-arrestins bind to a common binding site in the conserved PDE4 catalytic unit (Bolger et al., 2003). It also indicates that whatever differences there may be in the conformation of the catalytic unit of these PDE4A isoforms, as gauged from altered thermostability and inhibitor sensitivity, this does not extend to ablating interaction with β-arrestin2.

PDE4A11 is inhibited by a number of PDE4-selective inhibitors, including cilomilast (Ariflo) and roflumilast (Table 2), which are currently undergoing clinical trials (Timmer et al., 2002; Gamble et al., 2003; Spina, 2003). In this, we note that roflumilast is by far the most potent of these inhibitors, with an IC_{50} value some 150-fold lower than that of the archetypal PDE4 inhibitor rolipram (Table 2). We also show that there is no difference in the sensitivity of the particulate, compared with the soluble forms of PDE4A11 to inhibition by these compounds (Table 2). As seen with activity analyses, the conformational difference in particulate versus soluble PDE4A11 detected by thermostability studies does not extend to any effect on inhibitor action. PDE4A4B thus remains the only identified PDE4A isoform in which rolipram more potently inhibits the particulate enzyme compared with the cytosolic species (Huston et al., 1996; McPhee et al., 1999). We did observe some subtle differences in inhibition of these three PDE4A long isoforms. Thus, PDE4A11 is somewhat more sensitive to inhibition by Ariflo and denbufylline than either PDE4A4 or PDE4A10 (Table 2). Indeed, PDE4A11 and PDE4A10 are somewhat more sensitive to inhibition by Ro 20-1724 than PDE4A4 (Table 2). Furthermore, PDE4A10 is considerably less sensitive to inhibition by Ariflo, whereas it is considerably more sensitive to inhibition by rolipram than either PDE4A4 or PDE4A11 (Table 2).

The UCR1 regulatory module of all PDE4 isoforms contains a consensus site (RRESF) for phosphorylation by PKA. Studies done on PDE4D3, and later on other isoforms, showed that PKA phosphorylates the serine in this motif, causing enzyme activation (Sette and Conti, 1996; Hoffmann et al., 1998; MacKenzie et al., 2002). This has physiological significance in providing part of the cellular desensitization system to cAMP action (Oki et al., 2000). We have shown (Rena et al., 2001; MacKenzie et al., 2002) that PKA can phosphorylate PDE4 long isoforms from a variety of subfamilies, although activation is typically approximately 50%, compared with the 2- to 3-fold seen uniquely with PDE4D3 in which such amplification is presumed to be determined by the unique N-terminal region of PDE4D3. Here we show that in intact cells challenged with forskolin and IBMX so as to elevate intracellular cAMP levels, PDE4A11 is phosphorylated at Ser119 in UCR1, whereupon it is activated by approximately 80% (Fig. 9). This shows that PDE4A11 can also be regulated by PKA-mediated phosphorylation.

To begin to understand the role of PDE4 enzymes in cell biology and as therapeutic targets, it is crucial to appreciate the full range of isoforms. Here we have identified a novel, widely expressed PDE4A long isoform whose unique N-terminal region determines intracellular targeting and exerts a conformational action on this isoform that is clearly evident from the various differences noted here compared with other PDE4A long isoforms (Table 3). When cAMP levels are elevated in cells, PDE4A11 becomes phosphorylated and activated by PKA. This feature, together with its intracellular targeting, shows that PDE4A11 is poised to contribute to compartmentalized cAMP signaling and desensitization. Indeed, of all three known PDE4A long isoforms, it is transcripts for PDE4A11 that we show here to be the highest by far, compared with either PDE4A10 or PDE4A4, in cells associated with inflammatory responses, such as monocytes, macrophages, and eosinophils. This might suggest that PDE4A11 could provide a novel target in the future for therapeutics aimed at particular isoforms, such as those using small inducible RNA.

Acknowledgments

We thank Jennifer M. Wilson and Frank P. Maurio (GlaxoSmithKline) for their help with Taqman analyses.

References

Alfonso-Jaume MA, Mahimkar R, and Lovett DH (2004) Co-operative interactions between NFAT (nuclear factor of activated T cells) c1 and the zinc finger transcription factors Sp1/Sp3 and Egr-1 regulate MT1-MMP (membrane type 1 matrix metalloproteinase) transcription by glomerular mesangial cells. *Biochem J* **380:** 735–747.

Baillie GS, Huston E, Scotland G, Hodgkin M, Gall I, Peden AH, MacKenzie C, Houslay ES, Currie R, Pettitt TR, et al. (2002) TAPAS-1, a novel microdomain within the unique N-terminal region of the PDE4A1 cAMP-specific phosphodiesterase that allows rapid, Ca^{2+}-triggered membrane association with selectivity for interaction with phosphatidic acid. *J Biol Chem* **277:**28298–28309.

Baillie GS, MacKenzie SJ, McPhee I, and Houslay MD (2000) Sub-family selective actions in the ability of Erk2 MAP kinase to phosphorylate and regulate the activity of PDE4 cyclic AMP-specific phosphodiesterases. *Br J Pharmacol* **131:** 811–819.

Baillie GS, Sood A, McPhee I, Gall I, Perry SJ, Lefkowitz RJ, and Houslay MD (2003) beta-Arrestin-mediated PDE4 cAMP phosphodiesterase recruitment regulates beta-adrenoceptor switching from Gs to Gi. *Proc Natl Acad Sci USA* **100:**940–945.

Barber R, Baillie GS, Bergmann R, Shepherd MC, Sepper R, Houslay MD, and Heeke GV (2004) Differential expression of PDE4 cAMP phosphodiesterase isoforms in inflammatory cells of smokers with COPD, smokers without COPD and nonsmokers. *Am J Physiol* **287:**L332–L343.

Beard MB, Huston E, Campbell L, Gall I, McPhee I, Yarwood S, Scotland G, and Houslay MD (2002) In addition to the SH3 binding region, multiple regions within the N-terminal noncatalytic portion of the cAMP-specific phosphodiesterase, PDE4A5, contribute to its intracellular targeting. *Cell Signal* **14:**453–465.

Beavo JA and Brunton LL (2002) Cyclic nucleotide research—still expanding after half a century. *Nat Rev Mol Cell Biol* **3:**710–718.

Bolger G, Michaeli T, Martins T, St. John T, Steiner B, Rodgers L, Riggs M, Wigler M, and Ferguson K (1993) A family of human phosphodiesterases homologous to the dunce learning and memory gene product of *Drosophila melanogaster* are potential targets for antidepressant drugs. *Mol Cell Biol* **13:**6558–6571.

Bolger GB (1994) Molecular biology of the cyclic AMP-specific cyclic nucleotide phosphodiesterases: a diverse family of regulatory enzymes. *Cell Signal* **6:**851–859.

Bolger GB, McCahill A, Huston E, Cheung YF, McSorley T, Baillie GS, and Houslay MD (2003) The unique amino-terminal region of the PDE4D5 cAMP phosphodiesterase isoform confers preferential interaction with β-arrestins. *J Biol Chem* **278:**49230–49238.

Burnouf C and Pruniaux MP (2002) Recent advances in PDE4 inhibitors as immunoregulators and anti-inflammatory drugs. *Curr Pharm Des* **8:**1255–1296.

Chapman CG, Meadows HJ, Godden RJ, Campbell DA, Duckworth M, Kelsell RE, Murdock PR, Randall AD, Rennie GI, and Gloger IS (2000) Cloning, localisation and functional expression of a novel human, cerebellum specific, two pore domain potassium channel. *Brain Res Mol Brain Res* **82:**74–83.

Conti M, Richter W, Mehats C, Livera G, Park JY, and Jin C (2003) Cyclic AMP-specific PDE4 phosphodiesterases as critical components of cyclic AMP signaling. *J Biol Chem* **278:**5493–5496.

Gamble E, Grootendorst DC, Brightling CE, Troy S, Qiu Y, Zhu J, Parker D, Matin D, Majumdar S, Vignola AM, et al. (2003) Antiinflammatory effects of the phosphodiesterase-4 inhibitor cilomilast (Ariflo) in chronic obstructive pulmonary disease. *Am J Respir Crit Care Med* **168:**976–982.

Giembycz MA (2002) Development status of second generation PDE4 inhibitors for asthma and COPD: the story so far. *Monaldi Arch Chest Dis* **57:**48–64.

Hoffmann R, Wilkinson IR, McCallum JF, Engels P, and Houslay MD (1998) cAMP-specific phosphodiesterase HSPDE4D3 mutants which mimic activation and changes in rolipram inhibition triggered by protein kinase A phosphorylation of Ser-54: generation of a molecular model. *Biochem J* **333:**139–149.

Houslay MD (2001) PDE4 cAMP-specific phosphodiesterases. *Prog Nucleic Acid Res Mol Biol* **69:**249–315.

Houslay MD and Adams DR (2003) PDE4 cAMP phosphodiesterases: modular enzymes that orchestrate signalling cross-talk, desensitization and compartmentalization. *Biochem J* **370:**1–18.

Huston E, Beard M, McCallum F, Pyne NJ, Vandenabeele P, Scotland G, and Houslay MD (2000) The cAMP-specific phosphodiesterase PDE4A5 is cleaved downstream of its SH3 interaction domain by caspase-3. Consequences for altered intracellular distribution. *J Biol Chem* **275:**28063–28074.

Huston E, Pooley L, Julien P, Scotland G, McPhee I, Sullivan M, Bolger G, and Houslay MD (1996) The human cyclic AMP-specific phosphodiesterase PDE-46 (HSPDE4A4B) expressed in transfected COS7 cells occurs as both particulate and

cytosolic species that exhibit distinct kinetics of inhibition by the antidepressant rolipram. *J Biol Chem* **271:**31334–31344.
Johnston LA, Erdogan S, Cheung YF, Sullivan M, Barber R, Lynch MJ, Baillie GS, Van Heeke G, Adams DR, Huston E, et al. (2004) Expression, intracellular distribution and basis for lack of catalytic activity of the PDE4A7 isoform encoded by the human PDE4A cAMP-specific phosphodiesterase gene. *Biochem J* **380:**371–384.
Le Jeune IR, Shepherd M, Van Heeke G, Houslay MD, and Hall IP (2002) Cyclic AMP-dependent transcriptional up-regulation of phosphodiesterase 4D5 in human airway smooth muscle cells: identification and characterization of a novel PDE4D5 Promoter. *J Biol Chem* **277:**35980–35989.
MacKenzie SJ, Baillie GS, McPhee I, Bolger GB, and Houslay MD (2000) ERK2 MAP kinase binding, phosphorylation and regulation of PDE4D cAMP specific phosphodiesterases: the involvement of C-terminal docking sites and N-terminal UCR regions. *J Biol Chem* **275:**16609–16617.
MacKenzie SJ, Baillie GS, McPhee I, MacKenzie C, Seamons R, McSorley T, Millen J, Beard MB, van Heeke G, and Houslay MD (2002) Long PDE4 cAMP specific phosphodiesterases are activated by protein kinase A-mediated phosphorylation of a single serine residue in upstream conserved region 1 (UCR1). *Br J Pharmacol* **136:**421–433.
Maurice DH, Palmer D, Tilley DG, Dunkerley HA, Netherton SJ, Raymond DR, Elbatarny HS, and Jimmo SL (2003) Cyclic nucleotide phosphodiesterase activity, expression and targeting in cells of the cardiovascular system. *Mol Pharmacol* **64:**533–546.
McPhee I, Yarwood SJ, Huston E, Scotland G, Beard MB, Ross AH, Houslay ES, and Houslay MD (1999) Association with the SRC family tyrosyl kinase LYN triggers a conformational change in the catalytic region of human cAMP-specific phosphodiesterase HSPDE4A4B: consequences for rolipram inhibition. *J Biol Chem* **274:**11796–11810.
Mehats C, Jin SL, Wahlstrom J, Law E, Umetsu DT, and Conti M (2003) PDE4D plays a critical role in the control of airway smooth muscle contraction. *FASEB J* **17:**1831–1841.
Mongillo M, McSorley T, Evellin S, Sood A, Lissandron V, Terrin A, Huston E, Hannawacker A, Lohse MJ, Pozzan T, et al. (2004) Fluorescence resonance energy transfer-based analysis of cAMP dynamics in live neonatal rat cardiac myocytes reveals distinct functions of compartmentalized phosphodiesterases. *Circ Res* **95:**67–75.
Oki N, Takahashi SI, Hidaka H, and Conti M (2000) Short term feedback regulation of cAMP in FRTL-5 thyroid cells. Role Of pde4d3 phosphodiesterase activation. *J Biol Chem* **275:**10831–10837.
Ou XM, Chen K, and Shih JC (2004) Dual functions of transcription factors, transforming growth factor-β-inducible early gene $TIEG_2$ and Sp3, are mediated by CACCC element and Sp1 sites of human monoamine oxidase (MAO) B gene. *J Biol Chem* **279:**21021–21028.
Perry SJ, Baillie GS, Kohout TA, McPhee I, Magiera MM, Ang KL, Miller WE, McLean AJ, Conti M, Houslay MD, et al. (2002) Targeting of cyclic AMP degradation to β2-adrenergic receptors by β-arrestins. *Science (Wash DC)* **298:**834–836.
Perry SJ and Lefkowitz RJ (2002) Arresting developments in heptahelical receptor signaling and regulation. *Trends Cell Biol* **12:**130–138.
Rena G, Begg F, Ross A, MacKenzie C, McPhee I, Campbell L, Huston E, Sullivan M, and Houslay MD (2001) Molecular cloning and characterization of the novel cAMP specific phosphodiesterase, PDE4A10. *Mol Pharmacol* **59:**996–1011.
Sette C and Conti M (1996) Phosphorylation and activation of a cAMP-specific phosphodiesterase by the cAMP-dependent protein kinase. Involvement of serine 54 in the enzyme activation. *J Biol Chem* **271:**16526–16534.
Shepherd MC, Baillie GS, Stirling DI, and Houslay MD (2004) Remodelling of the PDE4 cAMP phosphodiesterase isoform profile upon monocyte-macrophage differentiation of human U937 cells. *Br J Pharmacol* **142:**339–351.
Spina D (2003) Phosphodiesterase-4 inhibitors in the treatment of inflammatory lung disease. *Drugs* **63:**2575–2594.
Sullivan M, Rena G, Begg F, Gordon L, Olsen AS, and Houslay MD (1998) Identification and characterization of the human homologue of the short PDE4A cAMP-specific phosphodiesterase RD1 (PDE4A1) by analysis of the human HSPDE4A gene locus located at chromosome 19p13.2. *Biochem J* **333:**693–703.
Terry R, Cheung YF, Praestegaard M, Baillie GS, Huston E, Gall I, Adams DR, and Houslay MD (2003) Occupancy of the catalytic site of the PDE4A4 cyclic AMP phosphodiesterase by rolipram triggers the dynamic redistribution of this specific isoform in living cells through a cyclic AMP independent process. *Cell Signal* **15:**955–971.
Timmer W, Leclerc V, Birraux G, Neuhauser M, Hatzelmann A, Bethke T, and Wurst W (2002) The new phosphodiesterase 4 inhibitor roflumilast is efficacious in exercise-induced asthma and leads to suppression of LPS-stimulated TNF-alpha ex vivo. *J Clin Pharmacol* **42:**297–303.
Vicini E and Conti M (1997) Characterization of an intronic promoter of a cyclic adenosine 3′,5′-monophosphate (cAMP)-specific phosphodiesterase gene that confers hormone and cAMP inducibility. *Mol Endocrinol* **11:**839–850.

Address correspondence to: Dr. Miles D Houslay, Molecular Pharmacology Group, Division of Biochemistry and Molecular Biology., Institute of Biomedical and Life Sciences, Wolfson Building, University Avenue, University of Glasgow, Glasgow G12 8QQ, Scotland, UK. E-mail: m.houslay@bio.gla.ac.uk